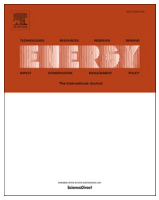
Energy 366 (2026) 142868



Contents lists available at ScienceDirect

Energy

journal homepage: www.elsevier.com/locate/energy





An integrated framework for evaluating tidal stream generation potential and its power system benefits: evidence from Great Britain

Daniil Hulak *, Marko Aunedi, Sobhan Naderian, Gareth Taylor

Brunel Interdisciplinary Power Systems Research Centre, United Kingdom

ARTICLE INFO

Keywords:
Tidal stream generation
Generator capacity expansion
GB power system
Power system simulation
Renewable energy

ABSTRACT

This paper presents an integrated framework that combines geospatial analysis with power system modelling to evaluate the optimal deployment and system-level value of tidal stream generation in Great Britain (GB). High-resolution geospatial screening – based on tidal maximum current velocity (≥2.5 m/s), mean tidal speeds (≥1.5 m/s) water depth (35–45 m and 30–50 m), and distance to shore (≤50 km) – is coupled with a multi-objective NSGA-II optimisation to identify Pareto-optimal sites for tidal stream development. The results indicate that promising locations are concentrated in a limited number of high-resource coastal regions, notably around the Orkney Islands and Pentland Firth, the Anglesey and North Wales coastline, and the Bristol Channel.

These sites are subsequently incorporated into a 17-zone representation of the 2030 GB electricity system using the PyPSA model. Simulation results show that deploying 1.5 GW of tidal stream capacity – on an energy-equivalent basis in place of wind and solar PV – reduces variable renewable curtailment by 0.6 TWh, displaces a comparable volume of gas-fired generation, and lowers total system operating costs by £65 million per year. Furthermore, analysis of electricity market impacts indicates reductions in average generation costs of up to £1.0/MWh in high-cost zones, alongside relatively stable technology-specific market capture prices for tidal stream generation compared to wind and solar.

The proposed framework is modular and scalable, making it applicable to other coastal regions and power systems using location-specific datasets and scenarios.

1. Introduction

Achieving Net Zero greenhouse gas emissions by 2050 has become a central objective of global energy policy, driving substantial structural changes across energy systems worldwide. This transition is already visible in volumes of renewable energy sources (RES) deployment. In 2024, nearly 585 GW of new RES capacity was added globally, representing an increase of around 15% compared to the previous year. Renewables were the dominant technology group in terms of new installations, accounting for 86% of all new electricity generation capacity installed in 2023 [1], 93% in 2024 [2] and 86% in 2025 [3].

However, RES deployment remains mostly focused on mature technologies. Solar Photovoltaic (PV) and onshore wind continue to lead global expansion, together accounting for over 95% of new renewable capacity added in 2024, with PV alone contributing more than 400 GW [4]. In contrast, ocean energy technologies, including tidal stream, tidal range, and wave power, remain at an early stage of technological and commercial maturity, with global installed capacity still below 1 GW, and only a limited number of commercial-scale projects in operation [5,6]. Although tidal energy offers high predictability relative to wind and solar generation, its current contribution remains limited, highlighting the need for a clearer understanding of its potential system value and integration pathways.

Similar trends in tidal energy deployment are observed in the United Kingdom (UK), despite its globally recognised tidal stream resource potential, estimated at around 11–16 GW of technically or practically extractable capacity according to recent assessments [7,8]. In 2024, the UK had approximately 58 GW of installed RES capacity, dominated by wind (31 GW) and solar PV (18 GW) [2], with total RES capacity rising to 65 GW in 2025 (a 12% increase), including growth in wind capacity to 33 GW and solar PV to 21 GW [3]. By comparison, the capacity of marine energy technologies is lower by several orders of magnitude, with operational projects totalling only around 10 MW [3], contributing a negligible share of the UK's renewable energy mix. Nevertheless, there are several tidal stream projects that have secured support through Contracts for Difference mechanism, including 41 MW in Allocation

* Corresponding author.
E-mail address: daniil.hulak@brunel.ac.uk (D. Hulak).

https://doi.org/10.1016/j.energy.2026.142868
Received 19 May 2026; Received in revised form 12 October 2026; Accepted 20 October 2026
Available online 21 October 2026
0360-5442/© 2026 The Authors. Published by Elsevier Ltd. This is an open access article under the CC BY license (http://creativecommons.org/licenses/by/4.0/).

Round 4 (AR) [9], 53 MW in AR5 [10], and 28 MW in AR6 [11], with delivery expected between 2026 and 2027. Furthermore, according to the Electricity Ten Year Statement 2024 (ETYS) [12] and Future Energy Scenarios 2025 (FES) documents [13], the UK plans to build or expand tidal energy generation to a projected capacity of around 0.6 GW by 2030.

To study the challenges and opportunities associated with a wider deployment of tidal stream technologies in the UK [14], this study develops a modelling framework that both identifies effective locations for tidal stream generation deployment and quantifies their system-level benefits for the power system of Great Britain (GB). The framework integrates high-resolution resource assessment based on Geographic Information Systems (GIS), multi-criteria spatial optimisation based on Non-dominated Sorting Genetic Algorithm II (NSGA II), and power system modelling to evaluate the contribution of tidal stream generation to system operation. The overall structure of the proposed framework is displayed in Fig. 1 and is described in detail in the Methodology section. This paper focuses specifically on tidal stream technology due to its comparatively lower installation, operational costs and shorter lead times [15].

The main contributions and novel aspects of this study can be summarised as follows:

- An integrated GIS-PyPSA framework is developed to link high-resolution tidal stream resource assessment with whole-system power system modelling for GB.
- A multi-objective NSGA II GIS spatial optimisation approach is applied to identify a constrained set of high-value tidal stream locations, jointly accounting for tidal current velocity, water depth, and proximity to the onshore transmission network.
- A novel 17-zone GB power system model, consistent with FES and the ETYS, is developed to quantify the operational and economic impacts of tidal stream integration under alternative deployment scenarios.

All the results of this research paper, including interactive maps, PyPSA code and the simulation results, are available via a GitHub repository [16].

The remainder of the paper is organised as follows. Section 2 reviews the state-of-the-art in tidal resource assessment and whole-system evaluation of marine energy integration. Section 3 outlines the proposed methodology, including the spatial allocation framework and the whole-system modelling approach applied to the GB power system. Section 4 presents and discusses the results, with a focus on the identification of optimal tidal stream deployment sites, comparison with existing studies, and the resulting implications for system operation and Net Zero pathways. Section 5 concludes the paper by summarising the

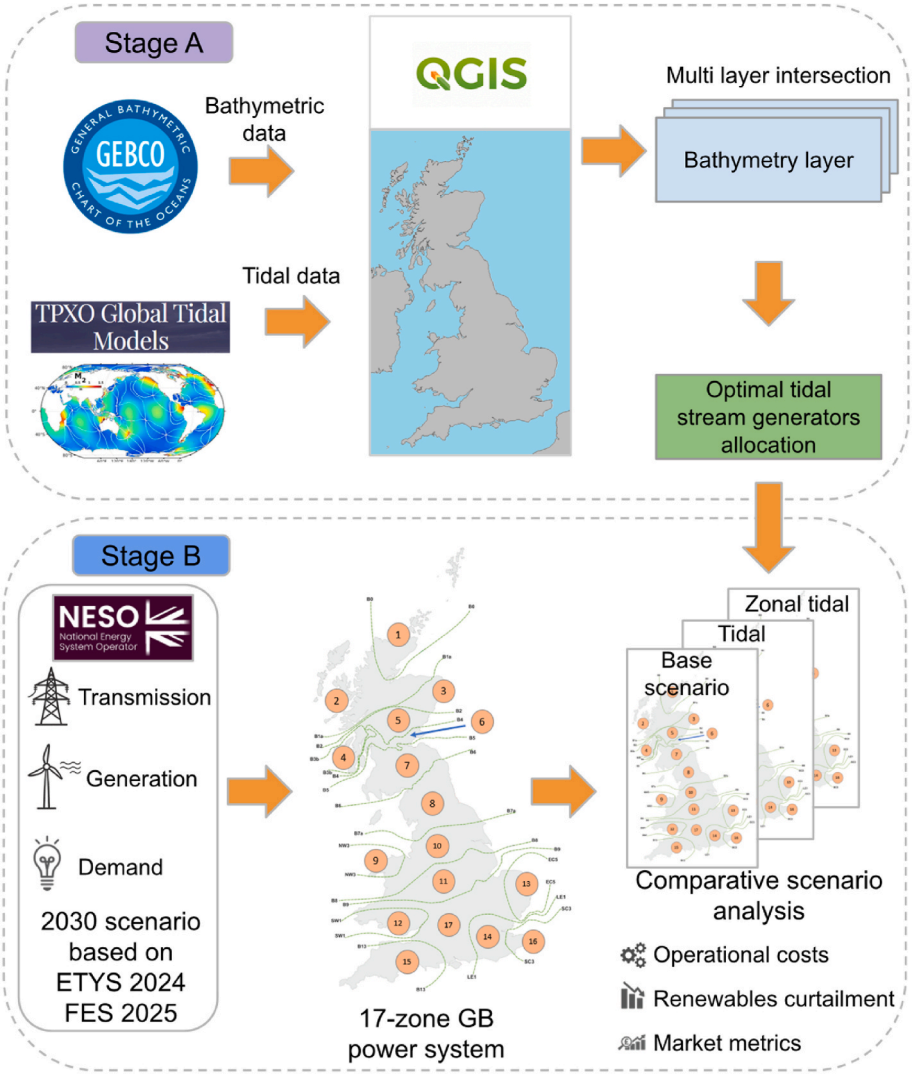


Fig. 1. Structure of the proposed framework.

key findings and highlighting directions for future research.

2. Review of the state-of-the-art

The accelerating transition towards Net Zero energy systems has intensified research interest in marine RES technologies, with tidal stream energy emerging as a promising, yet still developing, component of the future low-carbon electricity mix. Over the past two decades, research efforts have increasingly concentrated on improving the accuracy of tidal resource assessment [17–19], optimising device and array design [20–22], and evaluating system-level impacts through advanced power system modelling and techno-economic analysis [23,24].

To contextualise the structure and evolution of research on tidal stream technologies, a descriptive analysis of the academic literature is first conducted using the Scopus database [25,26]. This analysis examines publication trends and relationships across key research sub-topics, such as 'tidal stream', 'tidal stream resource', 'tidal stream power simulation', 'tidal stream UK', 'tidal stream generator performance', and 'tidal stream assessment'. The summary of the initial research literature analysis is presented in Fig. 2.

Fig. 2 shows an extensive growth in tidal stream research over the past two decades, with the number of publications increasing from fewer than 100 in the mid-2000s to more than 300 by 2025. Key sub-topics, including resource assessment, power system simulation, and generator performance, exhibit similar upward trends. While some fluctuations are evident across individual categories, the overall trajectory points to constantly increasing academic attention to tidal stream technology, with considerable contributions from regions such as the UK. The accompanying keyword cloud reinforces these observations, showing strong clustering trends around terms such as turbine, energy, current, model, and performance, which reflect the field's strong technical focus on device behaviour and energy capture. The presence of environmental and geographic terms such as estuary, coastal, and river, alongside methodological keywords including simulation, array, and analysis, indicates a progressively maturing and increasingly interdisciplinary research landscape. Taken together, the publication trends and keyword distribution suggest a field that is expanding and diversifying, while still exhibiting gaps in areas such as large-scale deployment analysis and techno-economic optimisation.

Across the literature, tidal stream resource assessments have been conducted for a wide range of national contexts, including the USA [27,28], Canada [29], France [30,31], China [32–34], South Korea [35–37], UK [14,19], Germany [38], and Vietnam [39,40]. The literature uses methods ranging from national GIS and tidal atlas screening to regional two- and three-dimensional hydrodynamic modelling and site-specific measurement campaigns. Common platforms include Finite Volume Community Ocean Model [28,29,33], TELEMAC [31] and MOHID [36]. Models are typically calibrated against tide-gauge, current-meter or Acoustic Doppler Current Profiler observations [28]. Array-scale studies also represent turbine energy extraction using enhanced-drag or momentum-sink terms [33]. Some research combines geospatial analysis in Quantum GIS (QGIS) [38] with bathymetric data from the General Bathymetric Chart of the Oceans (GEBCO) and tidal forcing derived from Oregon State University Tidal Inversion Model (TPXO) datasets [39]. These studies consistently demonstrate that tidal resources are highly spatially concentrated and that system-level benefits depend on targeted deployment at a limited number of high-energy sites rather than widespread installation across broader coastal areas [18,41].

From a resource quality perspective, a broad consensus has emerged with respect to the tidal velocity thresholds. Whereas peak velocities exceeding 2.5 m/s are widely regarded as commercially attractive and viable for energy extraction [42,43], there has been less consensus with respect to the mean speed criterion. In general terms, the relevant literature suggests that mean tidal current speeds below 1.5 m/s are generally considered insufficient for conventional tidal stream turbines [38]. A mean-magnitude threshold of 1.5 m/s can therefore be justified as a resource-persistence criterion. It prevents a site from qualifying solely because it experiences one brief high-speed peak while having weak velocities during the rest of the tidal cycle [18]. Using both mean and peak thresholds therefore distinguishes persistent high-flow locations from sites with short maximum values.

Although some variation exists in reported optimal installation depths, the literature suggests a relatively narrow range of preferred depths of between 20 and 50 m [43], with several studies proposing narrower intervals of 35–45 m [38] or an indicative depth of around 40

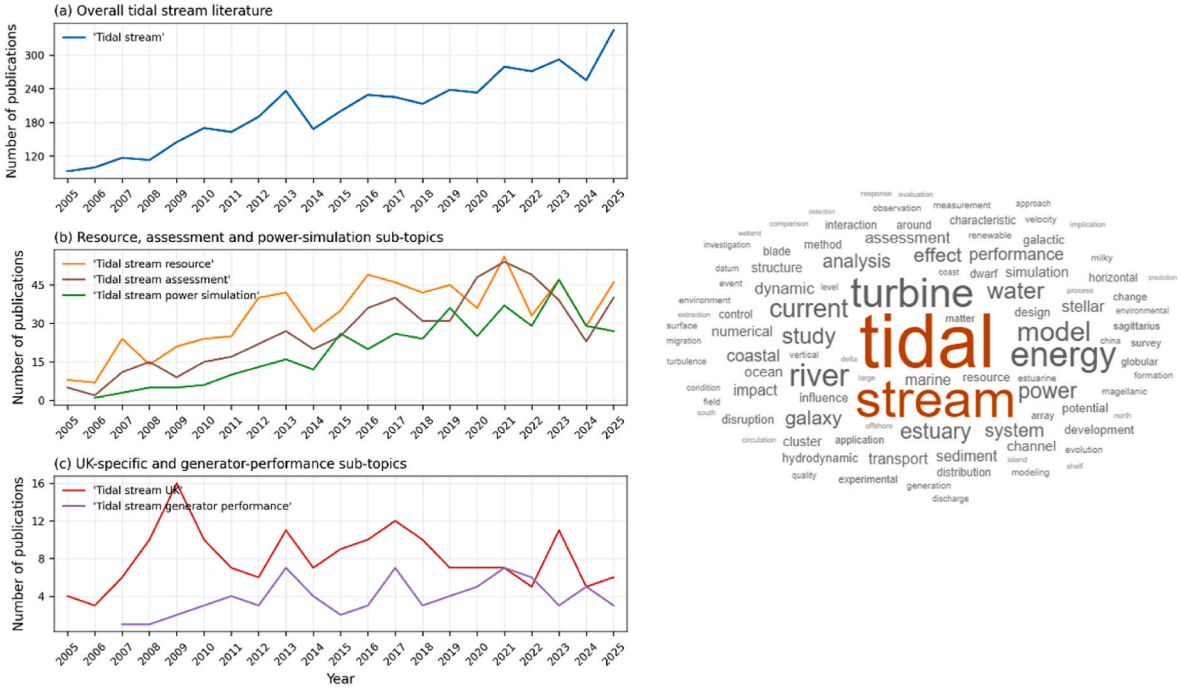


Fig. 2. Descriptive analysis of the tidal stream research papers trends (left) and papers' titles key words (right).

m [44,45]. These ranges reflect trade-offs between hydrodynamic performance, structural feasibility, and installation and monitoring requirements. Collectively, these findings define a set of physical constraints that underpin contemporary tidal stream site selection and inform the methodological assumptions adopted in this study.

The following three turbine technologies could be considered as potential candidates for deployment based on the criteria provided. MeyGen AR1500/HS1500, HydroQuest OceanQuest, and Nova M100-D represent different stages and scales of tidal stream technology. The AR1500 and HS1500 is a commercial scale installation, with 1.5 MW 18 m horizontal-axis rotors that have demonstrated long-term reliability under energetic UK tidal conditions [46]. Although the turbine reaches its rated power at approximately 3.0 m/s maximum tidal speed, it remains a relevant reference technology for this study because the adopted 2.5 m/s threshold is intended to identify areas with sufficiently strong tidal resources at the regional screening stage. The HydroQuest OceanQuest demonstrator closely matches the environmental conditions considered in this study (30–50 m water depth and 2.4–3.1 m/s max currents) [47]. It has bottom-mounted turbines that can operate within these conditions. The Nova M100-D demonstrates reliable operation in 30–40 m water depths and currents of around 2.6 m/s maximum tidal velocity, although its 100 kW capacity makes it more suitable as evidence of practical deployment and maintenance feasibility than as a representative commercial-scale technology [46].

A complementary strand of literature considers the contribution of tidal energy to the power system from a whole-system perspective. A key contribution in this area presents a modelling framework to quantify power system benefits of ocean energy deployment in GB using a whole-system optimisation approach [48]. The study utilises PyPSA as the core modelling Python library for power system analysis [49], representing the GB electricity system through a 9-zone network with a simplified topology, including generation, demand, storage, and inter-zonal transmission constraints. Input data are based on multiple sources, including FES, UK Government, and the Renewable Ninja platform [50,51]. The principal strength of this approach lies in its ability to quantify operational impacts, such as changes in dispatch patterns, balancing requirements, and system costs under increasing levels of ocean energy penetration. At the same time, the use of a simplified zonal representation imposes limitations on the spatial resolution of network constraints and regional effects.

Building on the previous research, this paper utilises established datasets and modelling tools while extending their application within an integrated framework tailored to the GB power system. Consistent with previous tidal resource assessments [14,19,52], TPXO tidal velocity data, GEBCO bathymetry [39], and QGIS-based spatial analysis [38] are used to identify candidate tidal stream sites. The key methodological advance lies in moving beyond threshold-based suitability screening by embedding the spatial analysis within a formal multi-objective NSGA II optimisation framework for tidal generator deployment. At the system level, the whole-system optimisation approach introduced by Ref. [48] is extended through an upgrade of the PyPSA network representation from 9 to 17 zones, aligned with ETYS boundaries and consistent with FES documents.

3. Methodology

3.1. Evaluation of potential tidal stream generator locations

The analysis of location-specific tidal stream generator deployment presented in this paper relies on findings from the research literature reviewed in the previous section, and is also informed by practical considerations relevant to tidal stream project development. To identify suitable locations for deployment, multiple scenarios are evaluated to reflect different characteristics discussed in the previous section. Collectively, these scenarios serve as a sensitivity analysis for site selection.

Firstly, locations characterised by average maximum tidal current velocities of at least 2.5 m/s are considered suitable for tidal stream generator deployment, in line with performance criteria reported in the literature [42]. Subsequently, the analysis is narrowed by applying a minimum average tidal current speed of 1.5 m/s to identify more robust, consistently high-flow locations rather than sites characterised only by short peak velocities [18]. Tidal current velocities are derived from the TPXO9-atlas-v5 data, following a methodology consistent with previous studies, while exploiting the improved spatial resolution and data assimilation capabilities of TPXO9-atlas-v5 relative to earlier releases such as TPXO8 [53–55]. The model incorporates major and minor astronomical tidal constituents, including M2, S2, N2, K2, 2N2, K1, O1, P1, Q1, Mf, Mm, M4, MN4, MS4, and S1, aligned with International Electrotechnical Commission Technical Specification (IEC TS) 62600-201 [56]. For this study, TPXO9-atlas-v5 outputs in 500 m × 500 m resolution are pre-processed in MATLAB using the 'scatteredInterpolant' function with natural-neighbour interpolation and extrapolation disabled. Received GeoTIFF rasters in the EPSG:27700 coordinate system capture tidal velocity fields across the GB domain. A QGIS, Cell Statistics and Zonal Statistics are then calculated along with temporal mean and maximum tidal velocities. In total, 960 hourly snapshots starting from 00:00 on 1 January are used to characterise tidal velocity conditions, covering a 40-day period, compliant with IEC TS 62600-201.

Secondly, consistent with engineering and deployment constraints, tidal stream generators are assumed to operate most effectively within a water-depth range of 35–45 m, with 40 m typically taken as the optimal reference depth for deployment. To assess the sensitivity of site selection to the permissible depth range, a broader range of 30–50 m is also considered. Accordingly, two depth scenarios are evaluated: 35–45 m and 30–50 m, with 40 m retained as the optimal reference depth in both cases. To represent this criterion spatially, bathymetric data from the GEBCO_2025 dataset [57] are used to construct the water depth layer, which is then processed to identify areas satisfying the specified depth range. GEBCO_2025 provides global bathymetric coverage at a spatial resolution of 15 arc-seconds, corresponding to around 500 m at the equator. The data are supplied in GeoTIFF format, enabling raster-based geospatial analysis through the inclusion of embedded georeferencing metadata.

Finally, to capture limitations related to grid connection, candidate sites are limited to those lying within 50 km of the shoreline, in order to ensure manageable cabling lengths and connection costs. While some previous studies adopted more conservative offshore distance limits of 20-35 km [58], this paper extends the threshold to 50 km to capture a wider set of technically feasible locations and to reflect potential future grid connection developments. Coastline contours for the GB case study are derived from GEBCO_2025 bathymetric data.

Spatial analysis is performed in QGIS [59], where the sea area surrounding the GB mainland is represented using a 500 m × 500 m grid. Major islands and peninsulas that are close to the GB mainland are also included in the analysis, as tidal stream generators located in their vicinity can be feasibly connected to the GB mainland power grid (this in particular includes areas surrounding the Isle of Wight, Anglesey, and the Orkney Islands).

Finally, once all spatial and technical constraints are defined, a multi-objective optimisation based on the NSGA-II algorithm [60] is applied to determine spatially optimised tidal stream generator locations [61]. The mathematical formulation of NSGA-II and its implementation using the PyMoo library [62] are described in detail in Section 3.3. The overall optimisation framework, encompassing site selection, connection constraints, and system integration, is illustrated in Fig. 3.

3.2. Optimising GB power system operation with tidal stream generation

In this paper, a 17-zone GB power system model is developed using

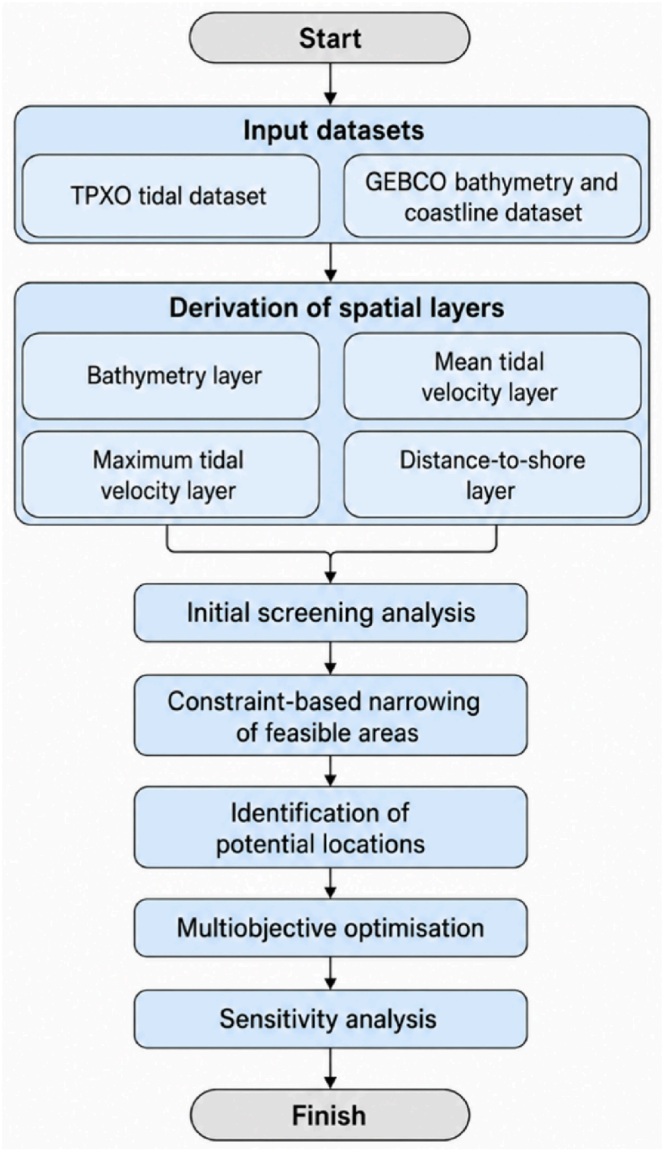


Fig. 3. Integrated optimisation framework for tidal stream generator siting and grid connection analysis.

the PyPSA modelling framework [49]. Parameters of the GB system model have been made consistent with the ETYS 2024 zonal boundaries and the 2030 planning horizon. Cross-zonal transmission capacities are taken directly from the ETYS 2024 Boundary Chart data [12] and reflect both existing transmission lines and committed network reinforcements.

Zonal electricity demand is constructed using the FES 2025 Holistic Transition 2030/2031 Winter Peak scenario [13] in combination with the regional demand breakdown. Minor FES regions are aggregated to ensure consistency with the 17 ETYS-aligned zones. To capture realistic temporal variability, an hourly national demand profile from the National Energy System Operator 2023 data portal [63] is applied and scaled to the 2030 Winter Peak level. Demand is then allocated across zones according to their respective regional shares.

The generation portfolio represents a 2030 system based on the ETYS 2024 Contracted Generation data [12] and FES 2025 Holistic Transition capacity projections [13]. Conventional generators are modelled with fixed installed capacities and constant marginal costs. Nuclear generators are assumed to operate as must-run units with a minimum output of 50% of installed capacity. Variable renewable generators (wind and solar PV) are represented using UK-representative hourly availability profiles that have been derived from Renewables Ninja [50,51], scaled by installed capacity, with site coordinates specified in Annex A. The hourly renewable generation profiles used in the simulations are presented in Fig. 4 as day–hour heatmaps. For each technology, the original 8760-h time series was reshaped into a 24 × 365 matrix, where the x-axis represents the day of the year and the y-axis represents the hour of the day. The colour scale represents the normalised hourly generation availability, or capacity factor, ranging from 0 to 1, where 0 indicates no available generation, and 1 indicates maximum available output relative to installed capacity. The tidal stream profile and generator marginal costs were adopted from Ref. [48], while the other renewable profiles were used to represent the temporal availability of offshore wind, onshore wind and PV generation in the GB system model. Detailed assumptions on generation and storage parameters are provided in Annex B.

Energy storage is represented through short-duration battery-type storage and pumped-hydro storage, with no direct marginal cost assigned to charging or discharging. Storage operation is therefore driven solely by system conditions, including demand levels, RES availability, and network constraints. Generic battery storage is modelled with a 2-h duration and symmetric charging and discharging efficiencies of 90%, and is initialised with zero stored energy. Pumped-hydro storage plants are represented with plant-specific power capacities, storage durations ranging from 4 to 20 h, and asymmetric efficiencies of 80% for charging and 93% for discharging [48]. These units are initialised at 50% of maximum energy capacity [64], ensuring immediate upward and downward flexibility at the start of the simulation.

Existing and planned interconnectors up to 2030 are included as capacity-constrained links, with technical data taken from Ref. [65]. System operation is simulated using PyPSA's linear optimal power flow (LOPF) [66] formulation over a full year at hourly resolution for the 2030 system. The resulting 17-zone GB power system representation and its corresponding single-line network topology are shown in Fig. 5.

Once suitable locations for tidal stream deployment had been identified and the GB power system model established, a set of tidal penetration scenarios was defined. The analysis begins with a baseline scenario in which no tidal generation is included. This is followed by a system-wide deployment scenario, where 0.5 GW of tidal stream capacity is introduced across all three suitable zones, replacing existing variable RES (wind and solar PV) generation on an energy-equivalent basis. In addition, a zone-by-zone sensitivity analysis is conducted, whereby tidal capacity is introduced individually in each suitable zone. This allows the identification of locations in which tidal stream deployment delivers the greatest system-level benefits.

Given that different RES technologies exhibit distinct temporal generation profiles, substitution is not performed on a simple capacity-equivalent basis. Instead, substitutions are balanced on an annual energy output basis to ensure comparable yearly generation. These coefficients are derived from the ratio of capacity factors, such that equivalent annual energy output is maintained across technologies. Specifically, the required installed capacity is scaled proportionally to the ratio between the tidal stream capacity factor and that of the substituted technology, similar to Ref. [67]. To achieve this, technology-specific substitution coefficients are applied, equal to 1.0 for onshore wind, 1.325 for offshore wind, and 0.3 for photovoltaic generation based on the differences in generation profiles. For instance, 0.5 GW of tidal stream generation with an annual capacity factor of 40% would nominally produce the same amount of electricity annually as 1.25 GW of solar PV capacity with a capacity factor of 12%, therefore, these ratios were taken into account when substituting wind and solar PV with tidal stream capacity across various scenarios.

To measure the contribution of tidal stream deployment to overall system performance, a range of model outputs are quantified: i) total electricity production, ii) system operation costs, iii) RES energy curtailment, iv) average generation costs, v) market capture price, and vi) weighted average electricity prices. The impact of tidal stream

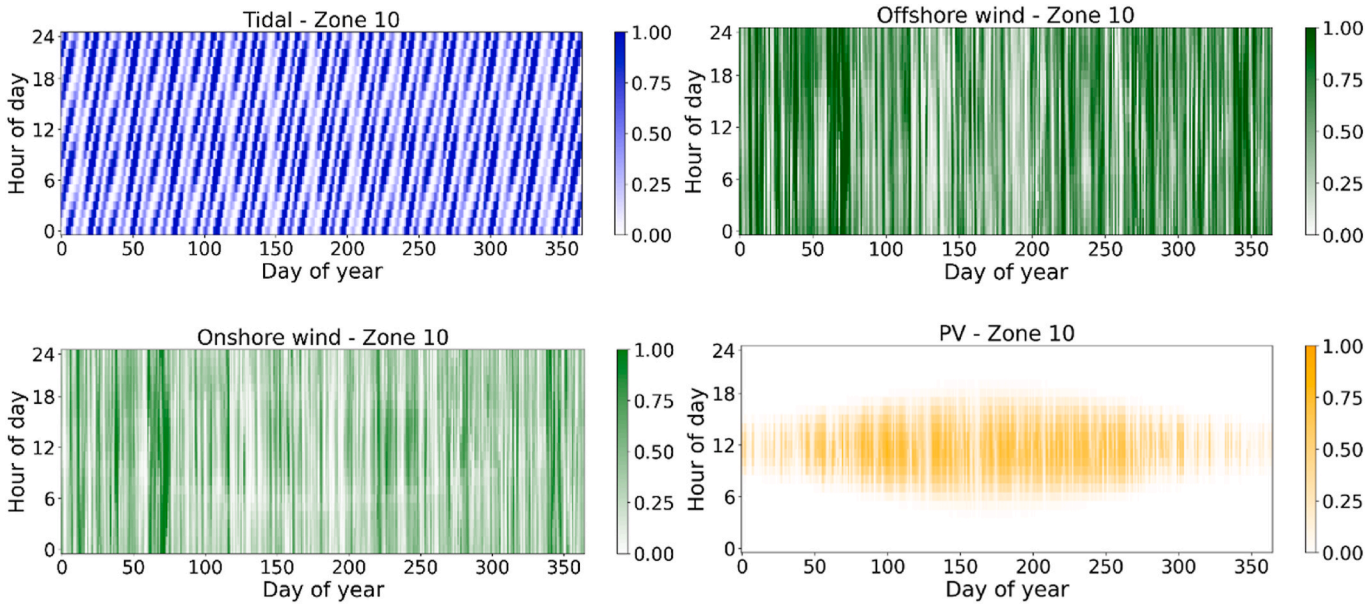


Fig. 4. Generation profiles of the RES used for the simulation.

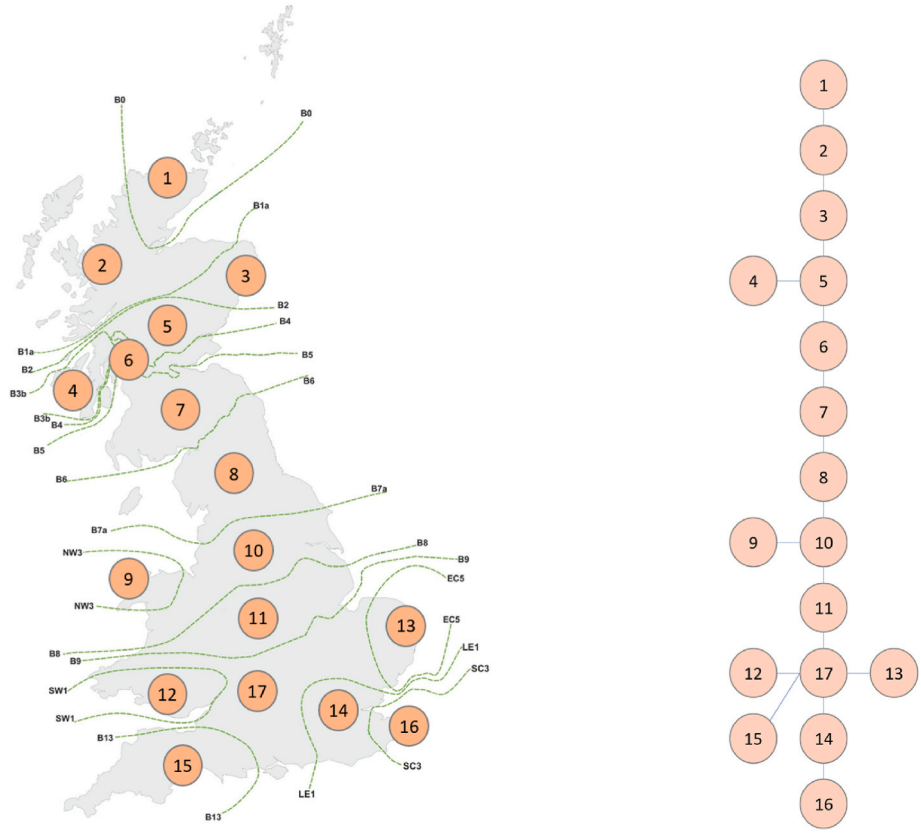


Fig. 5. 17-zone GB power system representation showing ETYS 2024 zonal boundaries (left) and the corresponding simplified single-line network topology used in the PyPSA model (right).

integration is assessed by comparing the values of these metrics to the baseline scenario, and quantifying the incremental system effects.

3.3. Software implementation of proposed framework

This study employs the open-source geographic information system QGIS [59] version 3.40.12 to identify and evaluate potential locations for tidal stream generator deployment. QGIS supports grid-based zonal analysis and enables the integration of multiple spatial data layers, allowing detailed assessment of bathymetric conditions and distance-to-shore constraints through the processing of GEBCO_2025 bathymetric data and tidal velocity fields derived from TPXO9-atlas-v5.

The QGIS-embedded tools used throughout the spatial analysis are summarised in Table 1. The table provides a concise description of each

Table 1
QGIS tools used for the analysis of tidal stream resource.

Layer	AP	AR	C	CG	CL	CR	CS	CT	DI	DN	F	GC	I	W	ZS
Bathymetry layer		■	■	■	■						■	■		■	■
Tidal speed layer		■	■			■	■				■	■			■
Distance layer								■	■	■	■	■			
Intersection layer												■	■		
Optimisation layer	■														

Where QGIS tools applied are: AP – add point layer, AR – add raster layer, C – clip, CG – create grid, CL – create layer, CR – clip raster by mask layer, CS – cell statistics, CT – centroids, DI – densify by interval, DN – distance to nearest hub (points), EV – extract vertices, F – filter, GC – graduated/categorised, I – intersection, W – warp (reproject), ZS – zonal statistics [68].

tool and its role in the workflow, with entries listed in alphabetical order for clarity and transparency.

Multi-objective site selection is implemented in Python using the PyMoo [62] version 0.6.1.6, with the NSGA-II algorithm [60] applied to identify Pareto-optimal [69] trade-offs between competing siting criteria. NSGA-II is a well-established multi-objective optimisation method, widely used for exploring complex, non-linear, and high-dimensional solution spaces while maintaining a well-distributed approximation of the Pareto front [69]. Unlike approaches that require a priori weighting of objectives, NSGA-II enables competing criteria to be treated explicitly and symmetrically, which is particularly appropriate for problems involving simultaneous technical, economic, and spatial considerations. As a result, the algorithm has been widely applied in power system simulations [70], RES integration [71], and geospatial optimisation studies [61], where trade-offs between resource quality, infrastructure distance, and site suitability are central.

Power system modelling is carried out using PyPSA [49] version 1.0.4, an open-source energy system modelling framework that supports linear optimal power flow (LOPF), unit commitment, and large-scale network analysis. PyPSA enables explicit representation of generator technical characteristics, including installed capacity, marginal costs, operational inflexibilities, storage behaviour, and inter-zonal transmission constraints. Its data structures allow for consistent time-series modelling of RES generation and demand. The PyPSA functions and components used in the power system modelling are summarised in Table 2.

The optimisation problems are solved using the CPLEX optimiser [72] version 22.1, integrated with Python 3.10. This configuration was found to provide stable and reliable performance for the 17-zone GB power system model. Across all scenarios, CPLEX consistently produced converged solutions and demonstrated robust handling of the large number of constraints associated with the high temporal and spatial resolution of the model.

Table 2
The shortlist of the function and components utilised to build a 17-zone GB power system.

Framework step	PyPSA function to implement
Initialise model	network = pypsa.Network()
Build network	network.add("Bus …") network.add("Load …") network.add("Generator …") network.add("Link …") network.add("StorageUnit …")
Run optimisation	network.optimize()
Extract and assess results	network.generators_t.p. network.storage_units_t.p. network.buses_t.marginal_price. network.links_t.p0. network.statistics.curtailment

3.4. Mathematical formulation of the proposed framework

3.4.1. Optimising locations for tidal stream generators

The optimisation problem for finding the best locations for tidal stream generators used in this paper is presented in equations (1)–(12). It integrates key spatial criteria to identify optimal tidal energy sites while observing the relevant constraints:

$$\min_{x\in\Omega_s} f_1(x) = \delta_P \tag{1}$$

$$\min_{x\in\Omega_s} f_2(x) = -v_P^{\max} \tag{2}$$

$$\min_{x\in\Omega_s} f_3(x) = -\bar{v}_P \tag{3}$$

$$\min_{x\in\Omega_s} f_4(x) = |d_P - 40| \tag{4}$$

$$\text{s.t. } g_1^{(s)}(x) = d_{\min}^{(s)} - d_P \le 0 \tag{5}$$

$$g_2^{(s)}(x) = d_P - d_{\max}^{(s)} \le 0 \tag{6}$$

$$g_3(x) = -v_P^{\max} + 2.5 \le 0 \tag{7}$$

$$g_4(x) = -\bar{v}_P + 1.5 \le 0 \tag{8}$$

$$x_i^L \le x_i \le x_i^U, i = 1, \ldots, 4 \tag{9}$$

$$x = \left[\delta_P, v_P^{\max}, \bar{v}_P, d_P\right] \in \Omega_s \tag{10}$$

$$\left(d_{\min}^{(1)}, d_{\max}^{(1)}\right) = (35, 45) \tag{11}$$

$$\left(d_{\min}^{(2)}, d_{\max}^{(2)}\right) = (30, 50) \tag{12}$$

where x is the vector of decision variables representing the geospatial attributes of a candidate site; δ_P is the distance to the shoreline; $v_P^{\max}$ is the maximum tidal current velocity; $\bar{v}_P$ is the mean tidal current velocity; and d_P is the water depth at the site. The objective functions $f_1(x)$, $f_2(x)$, $f_3(x)$, and $f_4(x)$ minimise the distance to the shoreline, maximise the maximum tidal velocity, maximise the mean tidal velocity, and minimise the deviation from the optimal reference depth of 40 m, respectively. The functions $g_1^{(s)}$ and $g_2^{(s)}$ define the permissible depth range under scenario s, while $g_3^{(s)}$ and $g_4^{(s)}$ require maximum and mean tidal velocities of at least 2.5 m/s and 1.5 m/s, respectively. Furthermore, x_i^L and x_i^U are the lower and upper bounds of the i-th decision variable, and Ω_s is the feasible solution space under depth scenario s, determined by

all relevant physical, environmental, and technical constraints. The optimisation is conducted separately for the two depth scenarios, with 40 m retained as the optimal reference depth in both cases.

In the proposed optimisation approach equations (1)–(4) define the four objective functions. Equation (1) minimises the distance to the shoreline, favouring sites that require lower cable lengths and are more accessible. Equations (2) and (3) maximise the maximum and mean tidal current velocities, respectively. Equation (4) minimises the absolute deviation of the site depth from the optimal reference depth of 40 m.

Equations (5) and (6) restrict the water depth to the lower and upper limits associated with scenario s. As specified by Equations (11) and (12), scenario 1 applies the narrower depth range of 35–45 m, whereas scenario 2 applies a broader range of 30–50 m; the optimal reference depth remains 40 m in both cases. Equations (7) and (8) require a maximum tidal current velocity of at least 2.5 m/s and a mean tidal current velocity of at least 1.5 m/s, respectively. Equation (9) imposes the lower and upper bounds on each decision variable, while equation (10) defines the complete decision vector.

NSGA-II is used to evolve a population of candidate solutions over successive generations using selection, crossover, and mutation. At each generation, individuals are ranked via fast non-dominated sorting, while solution diversity is preserved using a crowding-distance metric. Selection is performed through an elitist procedure that retains the best non-dominated and well-distributed solutions, forming the Pareto front. Mathematically, NSGA-II can be expressed as follows ([60,73]).

$P_t = \{x_1, x_2, \ldots, x_N\} \subset \Omega$ denotes the parent population at generation t. Q_t, the offspring population, is generated via genetic operators. The combined population is defined as:

$$R_t = P_t \cup Q_t \tag{13}$$

Solutions in R_t are partitioned using fast non-dominated sorting into a sequence of Pareto fronts:

$$\mathscr{F} = \{F_1, F_2, \ldots, F_K\} \tag{14}$$

where F_1 represents the set of non-dominated solutions and subsequent fronts correspond to increasing dominance levels. Within each front, a crowding-distance measure $\mathrm{CD}(x)$ is computed to quantify solution density in the objective space.

The next-generation population P_{t+1} is constructed through elitist selection according to Pareto rank and crowding distance:

$$P_{t+1} = \mathrm{Select}(\mathscr{F}, \mathrm{CD}) \tag{15}$$

$$|P_{t+1}| = N \tag{16}$$

This evolutionary process is repeated until a predefined termination criterion is satisfied, resulting in an approximation of the Pareto-optimal solution set that captures the trade-offs among the competing objectives defined.

3.4.2. Simulation of GB power system with tidal stream generators

To assess the operational behaviour of the GB power system under different tidal energy deployment levels, a simplified LOPF framework is applied. The model represents the hourly interaction of generation, storage, and cross-zonal electricity transfers over a full year in an hourly resolution. Power flows between zones are modelled using a transport-based abstraction, in which electricity can be exchanged up to predefined transfer capacities without the need to represent detailed electrical characteristics. The resulting mathematical structure forms the foundation for the optimisation described below:

$$\min_x \sum_{g \in G} c_g^{var} p_g \tag{17}$$

$$\text{s.t.} \sum_{g \in G_n} p_g + \sum_{s \in S_n} \left(p_s^{dis} - p_s^{ch}\right) + \sum_{l \in L_{n \to m}} f_l - \sum_{l \in L_{m \to n}} f_l = d_n, \forall n \in N \tag{18}$$

$$0 \le p_g \le \overline{P}_g, \forall g \in G \tag{19}$$

$$-\overline{F}_l \le f_l \le \overline{F}_l, \forall l \in L \tag{20}$$

$$0 \le p_s^{\mathrm{ch}} \le \overline{P}_s^{\mathrm{ch}}, 0 \le p_s^{\mathrm{dis}} \le \overline{P}_s^{\mathrm{dis}}, \forall s \in S \tag{21}$$

$$0 \le e_s \le \overline{E}_s, \forall s \in S \tag{22}$$

$$p_s^{\mathrm{dis}} - p_s^{\mathrm{ch}}, \forall s \in S \tag{23}$$

where p_g is the electrical output of the generator g, and c_g^{var} is its variable generation cost; p_s^{ch} and p_s^{dis} denote the charging and discharging power of the storage unit s, while e_s represents the energy stored in that unit at the current time step; f_l is the power flow on the transmission link l; d_n is the electricity demand in the zone n. The sets N, G, S, and L represent, respectively, the collection of zones, generators, storage units, and transmission links in the system, with $G_n \subseteq G$ and $S_n \subseteq S$ denoting the generators and storage units located in the zone n, and $L_{n \to m}$, $L_{m \to n}$ denoting links carrying flows between zones. $\overline{P}_g$ is the installed capacity of the generator g; $\overline{P}_s^{\mathrm{ch}}$ and $\overline{P}_s^{\mathrm{dis}}$ are the maximum charging and discharging rates of the storage unit s; $\overline{E}_s$ is its energy capacity; and $\overline{F}_l$ is the transfer capacity of the link l.

Equation (17) defines the objective function, which minimises the total variable generation cost of all generators included in the system. Equation (18) imposes the power balance requirement in every zone n, where electricity demand must be met by the sum of generation within the zone, the net contribution of storage, and net electricity exchanges through the interzonal links, according to the adopted flow-direction convention. The storage term is positive during discharging and negative during charging. Equation (19) limits the output of each generator to the range between zero and its installed capacity. Equation (20) constrains the power flow on each transmission link to its permitted transfer capacity in both directions. Equation (21) separately bounds the charging and discharging power of every storage unit by the corresponding maximum rates. Equation (22) ensures that the stored energy remains non-negative and does not exceed the energy capacity of the storage unit. Equation (23) represents the net storage power term used in the zonal balance: discharging delivers electricity to the system, whereas charging withdraws electricity from it. Together, Equations (13)–(19) describe a least-cost operating state in which zonal demand is satisfied while respecting generation, storage, and cross-zonal transfer limits.

The system performance metrics used for scenario evaluation are defined as follows.

The annual energy output of a generator technology k under scenario s is given by:

$$E_k^{(s)} = \sum_{t \in \mathscr{T}} w_t \sum_{g \in \mathscr{G}^{(k)}} p_{g,t}^{(s)} \tag{24}$$

Total system operating cost is calculated as:

$$C_{\mathrm{op}}^{(s)} = \sum_{t \in \mathscr{T}} w_t \sum_{g \in \mathscr{G}} c_g^{\mathrm{marg}} p_{g,t}^{(s)} \tag{25}$$

RES curtailment [74] is expressed as:

$$E_{\mathrm{curt}}^{(s)} = \sum_{t \in \mathscr{T}} w_t \sum_{r \in \mathscr{R}} \left(p_{r,t}^{\mathrm{avail},(s)} - p_{r,t}^{(s)}\right) \tag{26}$$

The average generation cost of the system is defined as:

$$\overline{c}_{\mathrm{gen}}^{(s)} = \frac{\sum_{t \in \mathscr{T}} w_t \sum_{g \in \mathscr{G}} c_g^{\mathrm{marg}} p_{g,t}^{(s)}}{\sum_{t \in \mathscr{T}} w_t \sum_{g \in \mathscr{G}} p_{g,t}^{(s)}} \tag{27}$$

The market capture price [75] for a given technology k is computed as:

$$\mathrm{MCP}_k^{(s)} = \frac{\sum_{t\in\mathscr{T}} w_t \pi_t^{(s)} \sum_{g\in\mathscr{G}^{(k)}} p_{g,t}^{(s)}}{\sum_{t\in\mathscr{T}} w_t \sum_{g\in\mathscr{G}^{(k)}} p_{g,t}^{(s)}} \tag{28}$$

The weighted average market [76] price is given by:

$$\overline{\pi}^{(s)} = \frac{\sum_{t\in\mathscr{T}} w_t \pi_t^{(s)} D_t^{(s)}}{\sum_{t\in\mathscr{T}} w_t D_t^{(s)}} \tag{29}$$

Differences between scenarios are evaluated as:

$$\Delta M^{(s)} = M^{(s)} - M^{(s_0)} \tag{30}$$

where $t \in \mathscr{T}$ denotes the set of modelled time steps, w_t the corresponding time-step weights, $p_{g,t}$ the dispatched power of generator g, c_g^{marg} the marginal generation cost, π_t the market price, D_t the system demand, $\mathscr{G}$ the set of all generators, $\mathscr{G}^{(k)}$ the subset of generators belonging to technology k, and $\mathscr{R}$ the set of RES energy sources.

Changes in these metrics are used to assess the system impacts of tidal stream deployment relative to the reference scenario. Increases in annual energy output E_k indicate a greater contribution of the corresponding technology to system supply, while reductions in total operating cost C_{op} and average generation cost $\overline{c}_{\mathrm{gen}}$ reflect improved economic efficiency. Lower RES curtailment E_{curt} signifies enhanced integration of variable RES and more effective utilisation of available resources. Higher market capture prices MCP_k indicate improved alignment of generation with high-price periods, whereas changes in the weighted average market price $\overline{\pi}$ reflect broader impacts on market outcomes.

4. Results and discussion

4.1. Optimal locations for tidal stream generation in the GB system

The multi-layer spatial screening framework described in the Methodology section was first used to identify candidate locations that satisfy

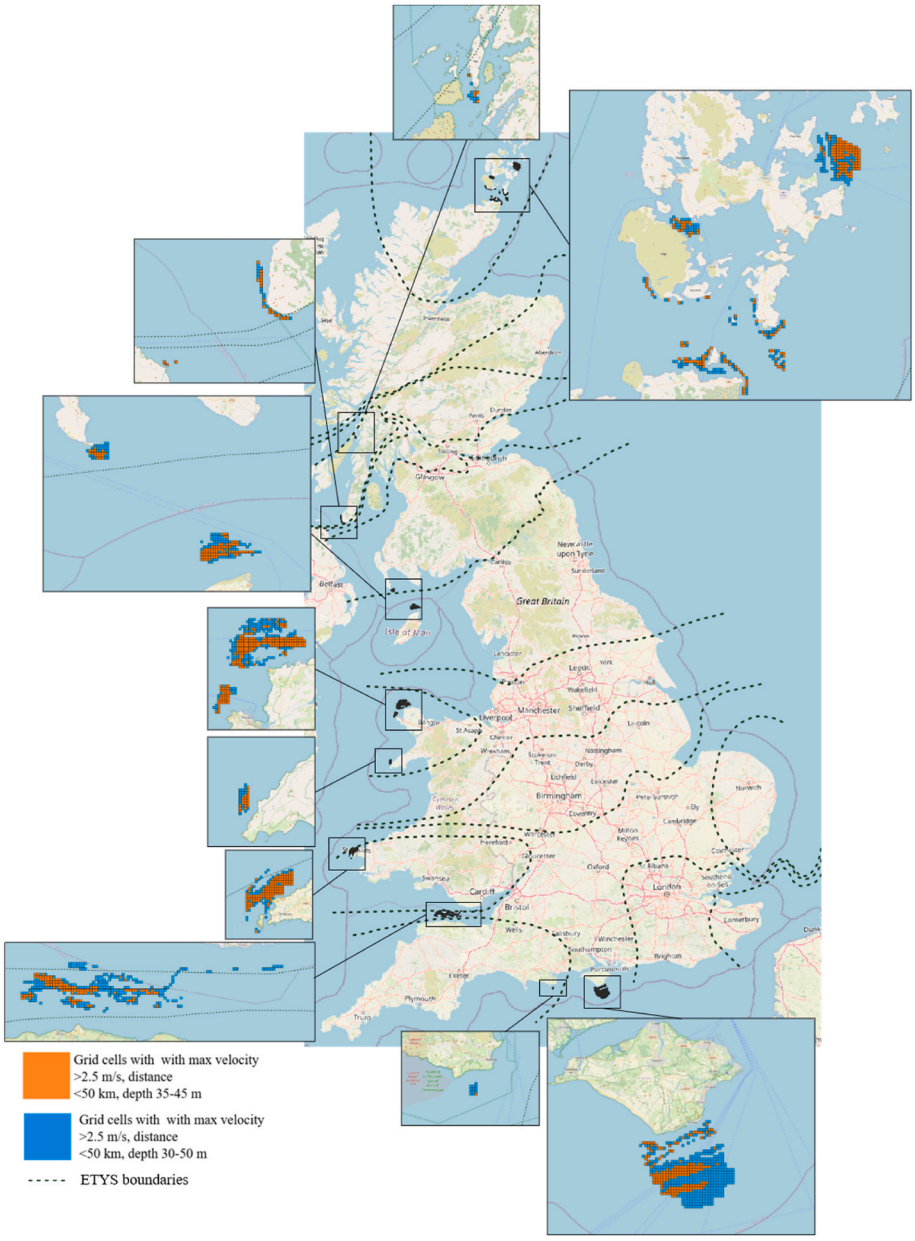


Fig. 6. Spatial distribution of tidal stream generator locations meeting the initial deployment criteria across key GB coastal zones. Geographical basemap: © OpenStreetMap contributors (openstreetmap.org/copyright).

the criteria of maximum tidal current velocity of 2.5 m/s, a distance to a candidate site within 50 km of the shoreline, water depth within the ranges of 35–45 m and broader 30–50 m. Each marker represents a 500 m × 500 m grid cell. As shown in Fig. 6, the intersection of the layers highlights several high-potential regions, in particular around the Orkney Islands and within the Pentland Firth channel between mainland Scotland and Orkney. Additional areas of interest are defined near the Isle of Anglesey, within the Bristol Channel, along the Welsh coastline near the Pembrokeshire Coast, and in the English Channel adjacent to the Isle of Wight.

These findings broadly align with the locations identified by previous research into the GB tidal stream potential [14,18,41]. Nevertheless, through simultaneous consideration of multiple technical and spatial constraints, the analysis presented here suggests a more selective and deployment-oriented set of viable locations, thereby reducing the overall number of candidate sites. Accordingly, Fig. 7 presents the locations identified using more selective criteria: a maximum tidal current speed of at least 2.5 m/s, a mean speed of at least 1.5 m/s, and a distance to shore of no more than 50 km, evaluated under two alternative depth ranges of 35–45 m and 30–50 m. OpenStreetMap was used as the geographical basemap to provide additional spatial context, including major cities, coastlines, and administrative boundaries [77]. Two map scales were applied to improve geographical clarity and the visibility of the identified locations: 1:3,500,000 for the overall GB map and 1:215,000 for the zoomed-in areas.

The initial results of the multi-layer spatial screening of candidate locations are then used as inputs into the NSGA II optimisation. The objective of this stage is to identify the best sites for tidal stream generator deployment by simultaneously maximising maximum and mean tidal current velocities, constraining water depth around its optimal value (40 m) for both depth ranges (35-45 m and 30-50 m), and minimising distance to shore to reduce grid connection costs. This optimisation-based filtering refines the initial set of feasible locations by explicitly capturing trade-offs between resource quality and the proximity to grid infrastructure.

The resulting optimal sites are shown in Fig. 8, corresponding to segments in Fig. 7. Each tile in Fig. 7 represents a 500 m × 500 m grid cell selected by the optimisation as part of the Pareto-optimal solution set. Relative to the initial multi-layer screening, the optimisation yields a substantially reduced number of locations, due to a more selective

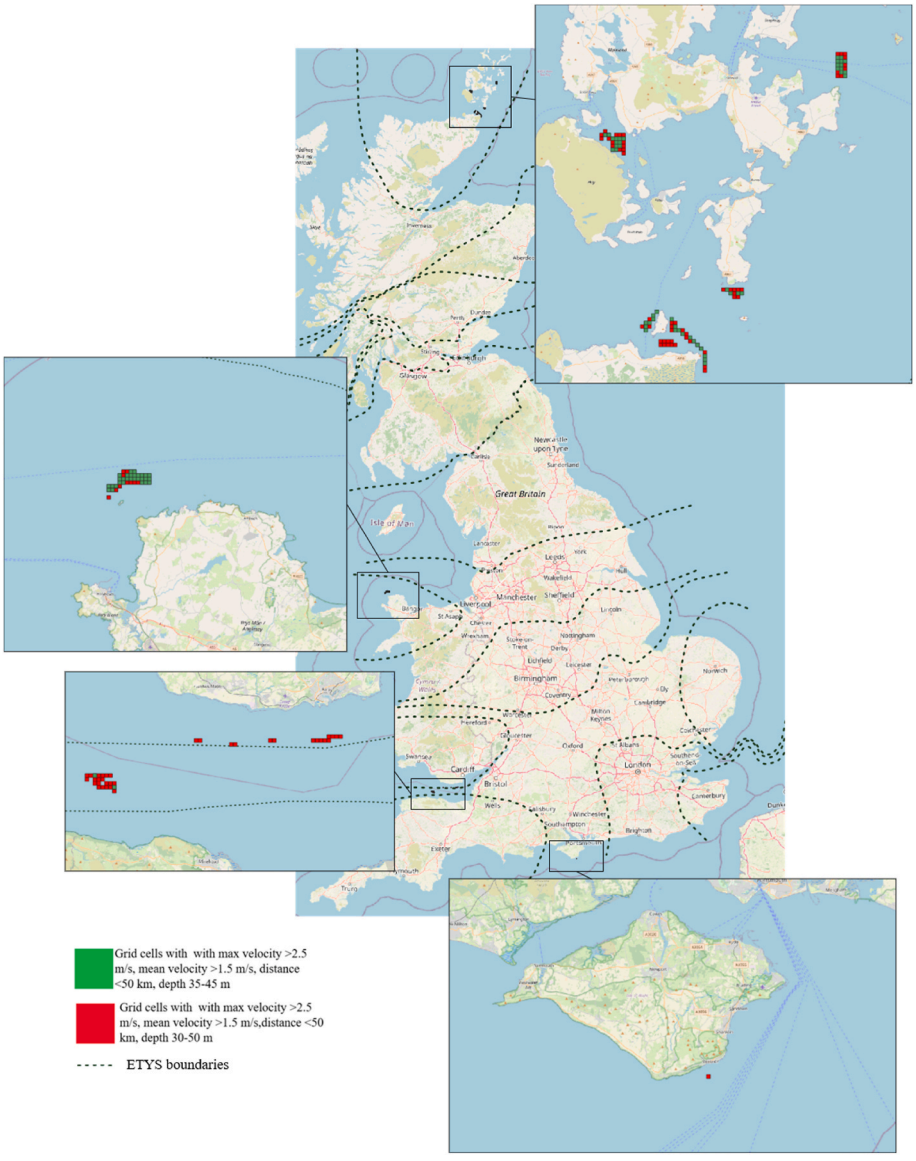


Fig. 7. Spatial distribution of tidal stream generator locations meeting advanced deployment criteria across key GB coastal zones. Geographical basemap: © OpenStreetMap contributors (openstreetmap.org/copyright).

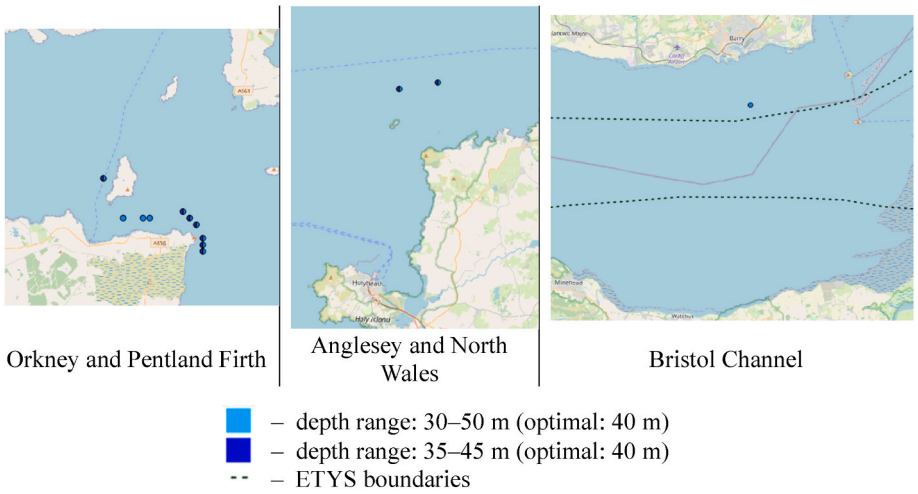


Fig. 8. Optimally selected tidal stream generator sites. Geographical basemap: © OpenStreetMap contributors (openstreetmap.org/copyright).

process that identifies those sites that outperform other sites across all criteria. Multiple scenarios considered an allowable depth range of 30–50 m, and subsequently a narrower range of 35–45 m, with 40 m specified as the optimal depth. All selected sites are suitable for connection to the GB mainland transmission grid and, when mapped onto the GB power system model used in this study (Fig. 5), the best locations are predominantly associated with zones 1, 9, and 15.

4.2. GB power system operation with tidal stream generators

Once the optimal spatial allocation of tidal stream generators has been established, the second part of the methodological framework addresses their system-level impacts on GB power system operation with high shares of variable renewable generation.

The generation capacity per technology as well as the minimum and maximum levels of demand are presented in Fig. 9 for each of the 17 zones used to represent the GB power system. The figure demonstrates there are significant differences in installed capacity and demand across the zones. For instance, zones 7, 10, 11, 13, and 17 have installed generation capacities that substantially exceed their peak demand, the surplus generation effectively making them potential net exporters under most operating conditions. In particular, zones 10 and 11 combine large-scale firm and variable generation with moderate local demand, positioning them as central supply hubs within the system. By contrast, some other zones such as zone 14 have a demand-generation imbalance, with peak demand approaching or exceeding the local capacity, implying a strong reliance on inter-zonal imports. At the system level, overall generation adequacy is maintained; however, a clear spatial mismatch between supply and demand necessitates substantial power transfers across zones.

The spatial configuration of the network and the associated cross-zonal transfer capacities shown in Fig. 10 indicate that the redistribution of surplus generation is constrained by several transmission corridors with restricted capacity that are likely to act as congestion points. In particular, north-south power transfers are effectively limited [78] by the capacities of the z7-z8 (10.2 GW) and z9-z10 (5.5 GW) corridors, restricting exports from northern surplus zones despite higher downstream capacities, such as the z10-z11 link (16.4 GW). Similarly, although major southern demand centres are connected to the rest of the system via high-capacity links (e.g. z14-z17 at 17.3 GW), the aggregate import capability of zone 17 is constrained by smaller upstream connections, including z12-z17 (2.9 GW) and z15-z17 (5.9 GW). These structural bottlenecks suggest that, even in the absence of aggregate generation scarcity, localised congestion is likely to arise, limiting the efficient utilisation of surplus RES generation.

Taken together, Figs. 9 and 10 allow for an initial comparative assessment of regional demand, installed generation capacity, and cross-zonal transfer capability. Building on this baseline characterisation, a set of LOPF simulations is carried out to evaluate a set of scenarios in which portions of baseline variable RES generation are progressively

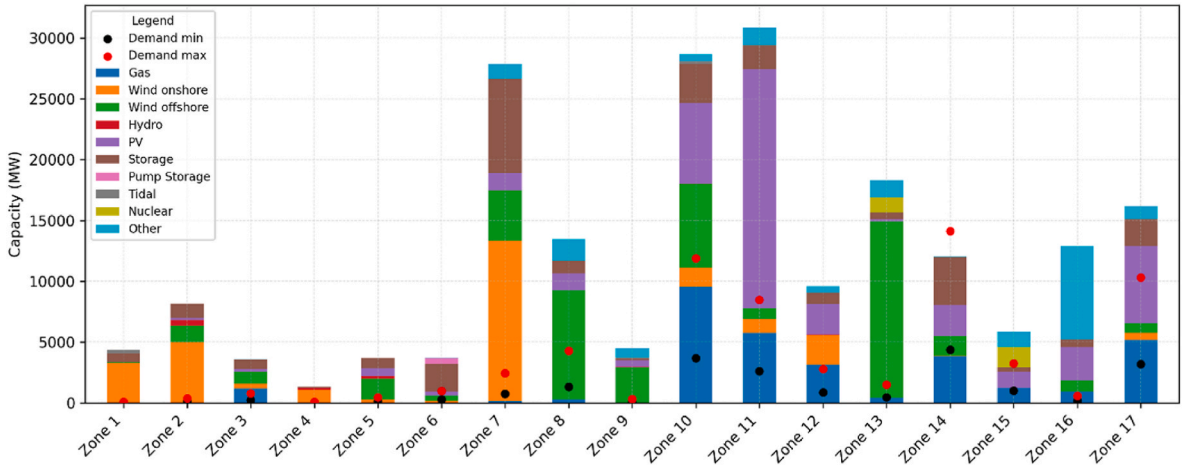


Fig. 9. Zonal generation capacity mix and demand bounds across the 17-zone GB power system.

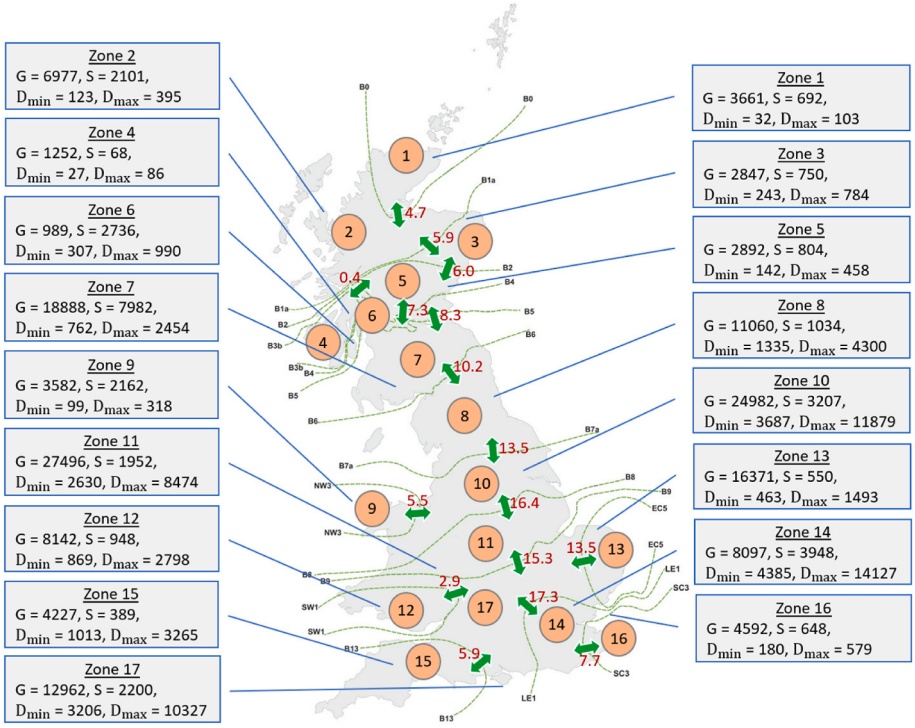


Fig. 10. Zonal generation, storage capacity, and transmission flows in the GB 17-zone power system, MW.

substituted with tidal stream generation.

Based on the analysis presented earlier in this section, zones 1, 9, and 15 in the GB power system model are identified as those with the most favourable conditions for tidal stream generator deployment. The baseline case represents the system configuration as specified in the FES and ETYS scenarios for 2030. In addition to this, a multi-zonal tidal deployment scenario is considered, in which 0.5 GW of tidal stream capacity is introduced in each of the three identified zones through the substitution of baseline renewable generation (i.e. wind and solar PV capacity).

To further investigate the spatial aspects of tidal stream integration, a set of additional zonal scenarios is evaluated, whereby 0.5 GW of tidal capacity is introduced individually in each zone. The corresponding adjustments to RES capacities and the associated tidal capacity additions applied under each scenario are described in Subsection 3.1 and summarised in Table 3. Owing to insufficient RES capacity within zone 15 to allow for full substitution, zone 12 is additionally included in the relevant scenarios and treated jointly with zone 15.

Fig. 11 illustrates changes in annual electricity generation and total system operating costs relative to the Baseline scenario following the integration of tidal stream generation. In the multi-zonal deployment case covering zones 1, 9, and 15, aggregate variable RES generation (wind, solar PV, and tidal stream) increases by approximately 0.6 TWh, referring to around 0.18% of total system demand of roughly 330 TWh. This additional RES output primarily displaces gas-fired generation, which decreases by about 0.5 TWh, equivalent to approximately 2.4% of baseline gas generation. Output from nuclear and other non-variable technologies remains largely unchanged. As a result, total system operating costs decline by nearly £65 million, representing a reduction of around 2.3% relative to the Baseline case. This cost reduction reflects the replacement of higher-marginal-cost thermal generation with low-marginal-cost and highly predictable tidal stream output.

It should be noted that the 0.6 TWh increase in the aggregate output of wind, PV and tidal generation is achieved despite the energy-equivalent substitution of wind and PV generation with tidal stream. In other words, the nominal annually available generation output from these three technologies is exactly the same in both cases. However, when tidal capacity replaces wind and PV, the aggregate RES curtailment reduces because the tidal output profiles offer better diversity when combined with the dominant wind and PV output patterns. As the result, a higher proportion of the available RES output is successfully integrated by the system, resulting in higher aggregate RES output.

The zonal sensitivity scenarios confirm the spatial robustness of these effects. Individual tidal stream deployment at the level of 0.5 GW in zones 1, 9, and 15 leads to expectedly smaller but consistent increases in variable RES generation, ranging from 0.14 to 0.24 TWh. These increases are accompanied by reductions in gas-fired generation of around 0.15-0.2 TWh and corresponding operating cost savings in the range of

Table 3
Scenario framework for tidal capacity integration and RES energy substitution with coefficients of 1.0 for onshore wind, 1.325 for offshore wind, and 0.4 for photovoltaic generation, MW.

Scenario	Zone 1	Zone 9	Zone 12, 15
Base scenario	-	-	-
Tidal zones 1, 9, 15	+500 tidal stream −100 wind onshore −302 wind offshore	+500 tidal stream −527 PV −258 wind offshore	+500 tidal stream −1310 PV - zone 15 −81 wind offshore - zone 12
Tidal zone 1	+500 tidal stream −100 wind onshore −302 wind offshore	-	-
Tidal zone 9	-	+500 tidal stream −527 PV −258 wind offshore	-
Tidal zone 15	-	-	+500 tidal stream −1310 PV - zone 15 −81 wind offshore - zone 12

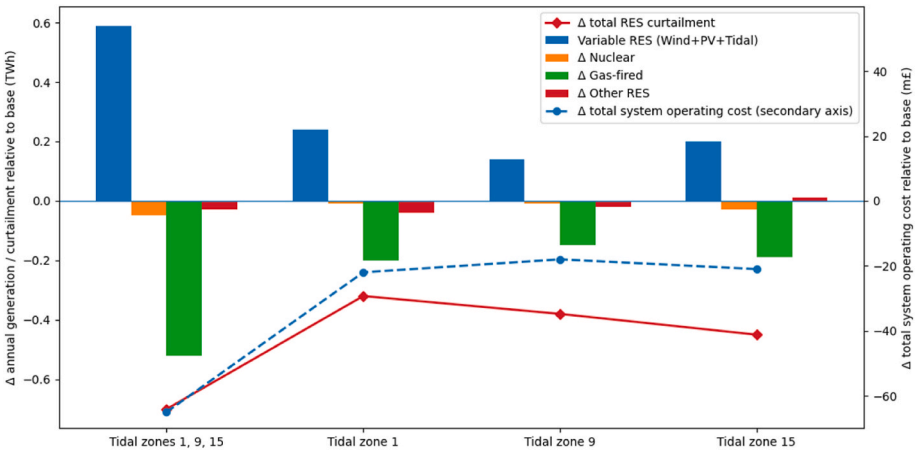


Fig. 11. Impact of tidal stream deployment on generation mix, RES curtailment, and system operating costs for the 17-zone GB power system.

£18-25 million. Taken together, these results indicate that geographically diversified tidal deployment delivers the largest system-wide economic benefits, while single-zone installations still provide consistent incremental cost reductions and displacement of thermal generation. This highlights the role of tidal stream generation as a complementary and system-supportive resource within the GB power system.

Fig. 11 also quantifies the impact of tidal stream integration on the overall variable RES curtailment. In the Baseline scenario, the total RES curtailment amounts to 85.84 TWh. The multi-zonal tidal deployment across zones 1, 9, and 15 delivers the largest reduction of RES curtailment, by about 0.69 TWh (around 0.8%). Individual zonal deployments achieve smaller reductions, ranging from 0.12 to 0.32 TWh. The greatest curtailment reductions also coincide with the corresponding increases in variable RES generation and the resulting displacement of gas-fired output, indicating a clear link between improved utilisation of zero-carbon and low-marginal-cost generation and reduced reliance on thermal dispatch. Across all scenarios, curtailment of tidal generation itself remains negligible, confirming a high level of system capability to absorb relatively modest volumes of tidal output. The observed relationship between reduced curtailment and operating cost savings suggests that geographically diversified tidal deployment can displace higher-cost generation as well as improve overall RES utilisation, while single-zone deployments provide smaller yet robust benefits.

4.3. *Impact of adding tidal stream generation on market prices*

Fig. 12 summarises the zonal and system-wide impacts of tidal deployment on the average generation cost, market capture price, and weighted average market price, capturing complementary dimensions of system performance that are relevant for policy design. The results show that tidal integration delivers its strongest local benefits in higher-cost zones, particularly zones 10-15, where average generation costs decline by up to approximately £0.8-1.0/MWh under the multi-zonal deployment scenario. These localised effects aggregate to a system-wide reduction in average generation cost of around £0.2/MWh,

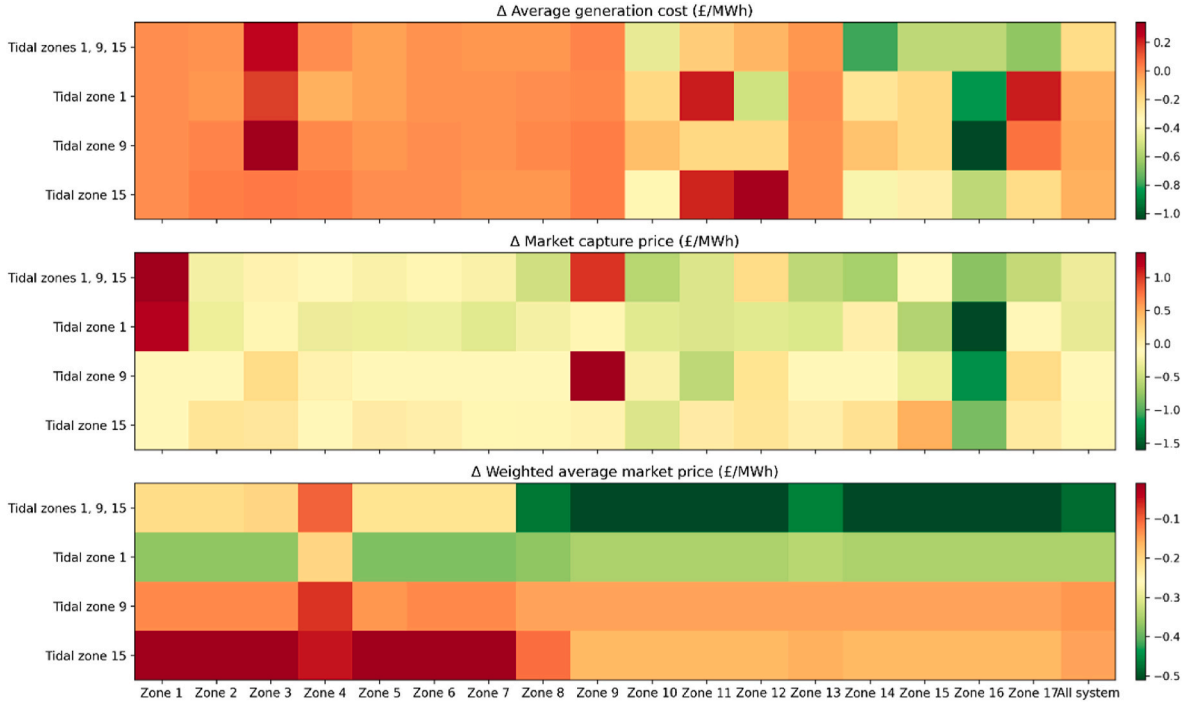


Fig. 12. Zonal impacts of tidal stream deployment on electricity prices and market metrics in the 17-zone GB power system.

indicating that tidal deployment can contribute to cost reductions at scale.

Market capture prices for the mix of RES show a greater level of spatial variation, with reductions of approximately £0.3-0.6/MWh in zones characterised by high RES penetration. This pattern reflects reduced price suppression and improved revenue stability for low-carbon generators. Despite this heterogeneity at the zonal level, the system-wide capture price consistently declines across all scenarios, suggesting that tidal stream integration improves aggregate market outcomes without materially weakening local investment signals.

Weighted average market prices decrease modestly but consistently across most zones, by approximately £0.2-0.5/MWh, indicating a price-smoothing effect that is directly relevant for consumer costs and overall market efficiency. Across all metrics, the multi-zonal deployment scenario delivers the largest and most spatially coherent benefits, while single-zone deployments yield smaller, more localised impacts. From a policy perspective, these findings support the role of tidal stream generation as a complementary RES technology that can reduce system operating costs, mitigate price volatility, and improve investment conditions when deployed in a coordinated and system-aware manner.

4.4. System integration cost of tidal stream generation

Based on the presented results of power system modelling it is also possible to quantify the System Integration Cost (SIC) of tidal stream generation. SIC of electricity generation technologies includes various categories of additional costs or benefits that are incurred in the system in addition to the levelised cost of building and operating the generation capacity itself [79]. SIC may include the impact on system balancing cost, cost of firm backup capacity, cost of reinforcing the grid infrastructure or the cost of maintaining system carbon emissions. SIC has been previously quantified using a whole-system approach [80] and by estimating its individual components [79–81].

Results for the system operation cost presented in this section allow for quantifying the SIC of tidal stream generation relative to a mix of wind and solar PV generation that is being replaced in the scenarios included in this analysis. Given that replacing wind and PV generation with tidal stream generation across all case studies resulted in cost reduction (as shown in Fig. 11), i.e., that the capacity replacement represented a net system benefit in terms of system operation cost, this will result in a negative value for SIC of tidal stream (or in other words, a system integration benefit).

The estimate of SIC provided in this section only includes operating cost, as this was included in the scope of the system optimisation model used in this paper. It is likely that optimising for other cost categories such as investment cost into generation, grid and energy storage infrastructure, may result in an even higher-magnitude system benefits of tidal stream power, although this needs to be confirmed by further research.

When calculating the SIC of a generation technology according to the method proposed in Ref. [80], it is important that any replacement of one generation technology with another is carried out using an energy-equivalent amount of capacity, i.e., that the removed and added capacities are capable of providing the same nominal annual output. Any resulting changes in total system cost, but excluding the Levelised Cost of Electricity (LCOE) of the technologies involved in the substitution, are then divided by the annual output of the added low-carbon technology to establish its relative SIC in £/MWh.

The estimated values of SIC for tidal stream generation, calculated across the four tidal zone scenarios used in this study, are shown in Table 4.

As discussed above, the SIC of tidal stream generation relative to a mix of wind and solar PV generation is found to be negative, suggesting that substituting a relatively small volume of tidal stream generation for variable wind and solar generation in a system that already has a high share of wind and solar results in a reduction in system cost. Taking as an example the SIC of tidal stream estimated at around −£14/MWh in the first scenario, this implies that when considering tidal stream as an investment candidate against renewable technologies such as wind and PV in this system, the LCOE of tidal can be up to £14/MWh higher than the LCOE of wind and solar PV, while still having the same overall cost effect when added to the system. In other words, the LCOE of tidal stream could include a premium with respect to wind and solar, while still being competitive with these technologies from the system perspective.

Table 4
Estimates of the SIC of tidal stream generation relative to wind and solar PV across tidal zone scenarios used in the study.

Criteria	Tidal zone scenario			
	Zones 1, 9, 15	Zone 1	Zone 9	Zone 15
SIC of tidal stream (£/MWh)	−13.9	−14.3	−11.0	−17.6

It can also be observed that the SIC benefit of tidal stream varies across different zones where this resource was assumed to be available, with the highest magnitude of system benefits observed in zone 15. This can be explained by the greater proximity of tidal stream generation in zone 15 to areas with high levels of demand (zones 14 and 17), reducing the effect of transmission grid constraints on transporting the tidal output towards the main demand centres.

5. Conclusions

This paper develops an integrated framework for assessing tidal stream deployment in GB by combining geospatial resource analysis, multi-objective optimisation, and whole-system power system modelling. By linking GIS-based site screening with an NSGA-II optimisation stage and a 17-zone, ETYS-consistent PyPSA model, the framework enables a system-aware evaluation of where tidal stream generation can deliver the greatest operational and economic value.

The results indicate that, once realistic physical and grid-connection constraints are applied, viable tidal stream deployment is spatially concentrated in a limited number of coastal regions, primarily associated with zones 1, 9, and 15 of the adopted GB grid model. Power system simulations demonstrate that integrating tidal stream generation increases the RES electricity output absorbed by the system, displaces gas-fired generation, and as the result reduces system operating costs and lowers the overall RES curtailment. These effects are most pronounced under geographically diversified deployment of tidal stream generation but remain robust across single-zone sensitivity scenarios. Analysis of price-based metrics further suggests that tidal stream generation gives rise to relatively stable market capture prices, supporting its role as a complementary technology within high-RES systems. Although the effect of adding tidal stream generation on prevailing market prices was observed to be relatively small due to the small volume of generation added to the system, the effects quantified through the System Integration Cost (SIC) were much more pronounced, with the system benefit of tidal stream relative to a mix of wind and solar PV generation estimated at £11-18/MWh.

The proposed framework can be scaled and transferred to other regions and power systems. Its modular structure allows the spatial screening, optimisation, and power system modelling components to be adapted to alternative datasets, network representations, and policy scenarios. As such, the framework provides a flexible decision support tool for assessing the system-level contribution of tidal stream generation within future low-carbon electricity systems.

Future work in this area will focus on including tidal stream generation into explicit generation investment optimisation models, as well as on explicit consideration of uncertainty related to variable RES generation technologies such as wind, in order to appropriately differentiate between stochastic wind output patterns and fully predictable tidal generation profiles.

Future work will also address the quantification of SIC against other low-carbon technologies such as nuclear, as well as a more comprehensive analysis of SIC by also quantifying its components related to investment cost into generation, storage and grid. Finally, future research will investigate the opportunities for deploying tidal stream generation technologies at lower tidal velocities (2 m/s and below) and different depths.

Finally, future research will also refine the annual energy production assessment by incorporating turbine-specific power curves, detailed array layouts, wake effects, turbine interactions and other array losses, thereby enabling estimation of net rather than gross annual energy production.

Nomenclature

Abbreviations, units	Definition
AR	Allocation Round
CfD	Contracts for Difference
CPLEX	IBM ILOG CPLEX Optimisation Studio
CPS	Capture Price for Solar
ETYS	Electricity Ten Year Statement
FES	Future Energy Scenarios
GB	Great Britain
GEBCO	General Bathymetric Chart of the Oceans
GIS	Geographic Information System
GW	Gigawatt
LCOE	Levelised Cost of Electricity
LOPF	Linear Optimal Power Flow
MCP	Market Capture Price
MW	Megawatt
NESO	National Energy System Operator
NSGA-II	Non-dominated Sorting Genetic Algorithm II
ORE	Offshore Renewable Energy
PV	Photovoltaic
PyMoo	Python Multi-Objective Optimisation library
PyPSA	Python for Power System Analysis
QGIS	Quantum Geographic Information System
RES	Renewable Energy Sources
SIC	System Integration Cost
TPXO	Oregon State University Tidal Inversion Model
TWh	Terawatt-hour
UK	United Kingdom

(*continued on next column*)

(*continued*)

CRediT authorship contribution statement

Daniil Hulak: Writing – original draft, Visualization, Software, Methodology, Investigation, Formal analysis. **Marko Aunedi:** Writing – review & editing, Supervision, Project administration, Methodology, Funding acquisition, Conceptualization. **Sobhan Naderian:** Writing – review & editing, Software. **Gareth Taylor:** Supervision, Resources.

Access to results datasets

The results generated in this study, including a complete set of QGIS-based spatial layers and PyPSA-based power system simulation code, are available online via GitHub repository [16].

Declaration of competing interest

The authors declare the following financial interests/personal relationships which may be considered as potential competing interests: Daniil Hulak reports financial support was provided by Gatsby Charitable Foundation. If there are other authors, they declare that they have no known competing financial interests or personal relationships that could have appeared to influence the work reported in this paper.

Acknowledgements

The research presented in this paper has been supported by the Gatsby Foundation.

Annex A

Site coordinates for the RES generators

Zone	PV		Wind onshore		Wind offshore	
	Latitude	Longitude	Latitude	Longitude	Latitude	Longitude
Zone 1	58.2999	−4.0361	58.2999	−4.0361	58.6566	−3.8483
Zone 2	57.3167	−4.5719	57.3167	−4.5719	56.9140	−6.0644
Zone 3	57.3770	−2.5348	57.3770	−2.5348	57.4630	−1.5746
Zone 4	55.9916	−5.5061	55.9916	−5.5061		
Zone 5	56.6068	−4.1142	56.6068	−4.1142	56.6333	−2.2711
Zone 6	56.2707	−3.2900	56.2707	−3.2900	56.3281	−2.4381
Zone 7	55.5565	−3.7055	55.5565	−3.7055	55.9529	−2.0524
Zone 8	54.6810	−2.5773			54.8540	−1.1515
Zone 9					53.1823	−4.5960
Zone 10	53.5076	−1.6702	53.5076	−1.6702	53.5296	0.3878
Zone 11	52.7090	−1.4613			53.2998	0.5317
Zone 12	51.7394	−3.3148	51.7394	−3.3148		
Zone 13	52.5518	1.3189			52.7255	1.8404
Zone 14	51.3393	0.2135			50.7188	−0.0847
Zone 15	50.8336	−3.8604				
Zone 16	51.2669	1.2394			51.2106	1.5025
Zone 17	51.8225	−1.2832			50.5874	−1.0368

Annex B

Assumed number and installed capacity of generation and storage assets (MW)

Generator type	Number of units	Minimum value	Maximum value	Average value	Median value	Total capacity
Biomass	6	15	396	98	42	588
Gas	76	6	2199	413	140	31368
Hydro	30	4	100	33	20	1001
Nuclear	2	1230	1670	1450	1450	2900
PV	196	16	1225	238	115	46688
Thermal	8	14	57	37	44	299
Tidal stream	3	100	287	199	210	597
Waste	3	40	83	58	50	173
Wind Offshore	68	10	3000	680	444	46216
Wind Onshore	303	5	660	96	69	29188
Pump Storage	6	210	1644	594	400	3566
Energy Storage System	163	8	1400	175	57	28605
Total	864					191188

Data availability

The results generated in this study, including a complete set of QGIS-based spatial layers and PyPSA-based power system simulation code are available online via GitHub repository.

References

[1] International Renewable Energy Agency (IRENA). Renewable capacity statistics 2024. 2024 [Online]. Available: irena.org/Publications/2024/Mar/Renewable-Capacity-Statistics-2024, [Accessed 15 April 2026].

[2] International Renewable Energy Agency (IRENA). Renewable capacity statistics 2025. 2025 [Online]. Available: www.irena.org. [Accessed 15 April 2026].

[3] International Renewable Energy Agency (IRENA). Renewable capacity statistics 2026. 2026 [Online]. Available: www.irena.org. [Accessed 15 April 2026].

[4] Diren Kocakuşak, Janna Smith, Kasandra O'Malia. Wind and solar year in review 2024. 2025 [Online]. Available: https://globalenergymonitor.org/wp-content/uploads/2025/01/GEM-briefing_-2024-wind-and-solar-year-in-review-Feb-2025.pdf. [Accessed 18 November 2025].

[5] Anatoli Chatzipanagi, et al. Clean energy technology observatory: photovoltaics in the european Union-2024 status report on technology development. Trends, Value Chains and Markets'; 2024 [Online]. Available: https://publications.jrc.ec.europa.eu/repository/handle/JRC139297. [Accessed 19 April 2026].

[6] International Renewable Energy Agency (IRENA). 'Ocean energy data' [Online]. Available: https://www.irena.org/Energy-Transition/Technology/Ocean-energy. [Accessed 15 April 2026].

[7] Offshore Renewable Energy (ORE) Catapult [Online]. Available: Tidal Stream Technology Roadmap'; 2024. https://cms.ore.catapult.org.uk/wp-content/uploads/2024/03/ORE-Catapult-Tidal-stream-roadmap-report-2024.pdf. [Accessed 19 November 2025].

[8] Tidal Stream Industry Energiser (Tiger). Cost reduction pathway of tidal stream energy in the UK and France. Accessed: Nov. 19, 2025. [Online]. Available: https://cms.ore.catapult.org.uk/wp-content/uploads/2022/10/Tidal-stream-cost-reduction-report-T3.4.1-v1.0-for-ICOE.pdf; 2022.

[9] Department for Energy Security and Net Zero (DESNZ). Contracts for difference (CfD) allocation round 4 results. 2022 [Online]. Available: https://assets.publishing.service.gov.uk/media/65b1463d160765000d18f834/contracts-for-difference-cfd-allocation-round-4-results.pdf. [Accessed 4 July 2025].

[10] Department for Energy Security and Net Zero (DESNZ). 'Contracts for difference allocation round 5 results', 2023 [Online]. Available: https://assets.publishing.service.gov.uk/media/64fa0473fdc5d10014fce820/cfd-ar5-results.pdf. [Accessed 4 July 2025].

[11] Department for Energy Security and Net Zero (DESNZ). 'Contracts for difference allocation round 6 results', 2024 [Online]. Available: https://assets.publishing.service.gov.uk/media/66d6ad7c6eb664e57141db4b/Contracts_for_Difference_Allocation_Round_6_results.pdf. [Accessed 4 July 2025].

[12] National Grid ESO/NESO. Electricity ten year statement 2024. 2024 [Online]. Available: https://www.neso.energy/publications/electricity-ten-year-statement-etys/etys-documents-and-appendices. [Accessed 19 November 2025].

[13] National Energy System Operator (NESO). Future Energy Scenarios (FES) 2025: 2025 [Online]. Available: https://www.neso.energy/publications/future-energy-scenarios-fes/fes-documents. [Accessed 15 January 2026].

[14] Pudjianto D, Frost C, Coles D, Angeloudis A, Smart G. UK studies on the wider energy system benefits of tidal stream. Energy Adv 2023;2. https://doi.org/10.1039/d2ya00251e.

[15] Shetty C, Priyam A. A review on tidal energy technologies. Mater Today Proc Jan. 2022;56:2774–9. https://doi.org/10.1016/J.MATPR.2021.10.020.

[16] GB-tidal-energy/README.md at GitHub repository [Online]. Available: https://github.com/Danielckua/gb-tidal-energy/blob/main/README.md. [Accessed 12 October 2026].

[17] Alday M, Lavidas G. Assessing the tidal stream resource for energy extraction in The Netherlands. Renew Energy Jan. 2024;220:119683. https://doi.org/10.1016/J.RENENE.2023.119683.

[18] Coles DS, et al. A review of global tidal stream energy resources. Proc R Soc A Dec. 2025;481(2328). https://doi.org/10.1098/RSPA.2024.0841.

[19] Thiébaut M, Sentchev A. Tidal stream resource assessment in the dover strait (eastern English Channel). Int J Mar Energy Dec. 2016;16:262–78. https://doi.org/10.1016/J.IJOME.2016.08.004.

[20] bin Abul Kashem S, Majid ME, Tabassum M, Ashraf A, Guziński J, Łuksza K. A preliminary study and analysis of tidal stream generators. Acta Energetica 2020:6–22.

[21] Gkantou Michaela et al., 'Offshore floating modular energy islands: technologies and challenges', J Phys Conf. doi: 10.1088/1742-6596/2896/1/012019.

[22] Touimi K, Benbouzid M, Chen Z. Optimal design of a multibrid permanent magnet generator for a tidal stream turbine. Energies Jan. 2020;13(2):487. https://doi.org/10.3390/EN13020487. 2020, Vol. 13, Page 487.

[23] Lewis M, et al. Power variability of tidal-stream energy and implications for electricity supply. Energy Sep. 2019;183:1061–74. https://doi.org/10.1016/J.ENERGY.2019.06.181.

[24] Coles DS, Adcock TAA. Assessment of tidal stream power's ability to enhance energy system resilience. Proc Euro Wave Tidal Energy Conf Sep. 2025;16:751–2. https://doi.org/10.36688/EWTEC-2025-751.

[25] Guz AN, Rushchitsky JJ. Scopus: a system for the evaluation of scientific journals. Int Appl Mech Oct. 2009;45(4):351–62. https://doi.org/10.1007/S10778-009-0189-4. 2009 45:4.

[26] Yakushev O, Hulak D, Zakharova O, Kovalenko Y, Yakusheva O, Chernyshov O. Management of the modern electric-vehicle market. Polityka Energetyczna – Energy Policy Journal 2022;25(2):85–108. https://doi.org/10.33223/epj/147694.

[27] Kilcher L, Haas K, Muscalus A. Tidal resource gaps analysis technical report [Online]. Available: https://www.nrel.gov/docs/fy23osti/86692.pdf. [Accessed 7 August 2026].

[28] Wang T, Yang Z. A tidal hydrodynamic model for Cook Inlet, Alaska, to support tidal energy resource characterization. J Mar Sci Eng Apr. 2020;8(4):254. https://doi.org/10.3390/JMSE8040254. 2020, Vol. 8, Page 254.

[29] Yang Z, et al. Modeling assessment of tidal energy extraction in the Western passage. J Mar Sci Eng Jun. 2020;8(6):411. https://doi.org/10.3390/JMSE8060411. 2020, Vol. 8, Page 411.

[30] Campbell R, Martinez A, Letetrel C, Rio A. Methodology for estimating the French tidal current energy resource. Int J Mar Energy Sep. 2017;19:256–71. https://doi.org/10.1016/J.IJOME.2017.07.011.

[31] Thiébot J, et al. Numerical modelling of hydrodynamics and tidal energy extraction in the Alderney race: a review: modelling the Alderney race: a review. Philos Trans R Soc A Math Phys Eng Sci Aug. 2020;378(2178). https://doi.org/10.1098/RSTA.2019.0498/41104.

[32] Dai P, Huang Z, Zhang J. A modelling study of the tidal stream resource around Zhoushan Archipelago, China. Renew Energy Dec. 2023;218:119234. https://doi.org/10.1016/J.RENENE.2023.119234.

[33] Wu H, Yu H, Fang Y, Zhou Q, Zhuo F, Kelly RM. Assessment of the tidal current energy resources and the hydrodynamic impacts of energy extraction at the PuHu channel in Zhoushan Archipelago, China. J Ocean Univ China Jun. 2021;20(3):478–88. https://doi.org/10.1007/S11802-021-4767-3.

[34] Liu X, et al. A review of tidal current energy resource assessment in China. Renew Sustain Energy Rev Jul. 2021;145:111012. https://doi.org/10.1016/J.RSER.2021.111012.

[35] Ko DH, Park JS, Lee KS. 'Assessment of Tidal Current Energy Potential at Uldolmok in the Southwestern Coast of Korea', vol. 85; May 2018. p. 1301–5. https://doi.org/10.2112/SI85-261.1. no. sp1 10.2112/SI85-261.1.

[36] Park JS, Lee CY, Park JS, Choi HW, Ko DH, Lee JL. Assessment of tidal stream energy resources using a numerical model in Southwestern Sea of Korea. Ocean Sci J Dec. 2019;54(4):529–41. https://doi.org/10.1007/S12601-019-0038-2.
[37] jin Hwang S, Jo CH. Tidal current energy resource distribution in Korea. Energies Nov. 2019;12(22):4380. https://doi.org/10.3390/EN12224380. 2019, Vol. 12, Page 4380.
[38] Korte A, Windt C, Goseberg N. Review and assessment of the German tidal energy resource. J Ocean Eng Marine Energy Dec. 2023;10(1):239–61. https://doi.org/10.1007/S40722-023-00309-7. 2023 10:1.
[39] Tran NH, Le AT, Nguyen QT, Tran HH, Tran PQ. Tidal current energy resource assessment for Vietnam. Conference proceedings - 2023 IEEE Asia meeting on environment and electrical engineering, EEE-AM. 2023. https://doi.org/10.1109/EEE-AM58328.2023.10395159. 2023.
[40] Camenen B, et al. Monitoring discharge in a tidal river using water level observations: application to the Saigon River, Vietnam. Sci Total Environ Mar. 2021;761:143195. https://doi.org/10.1016/J.SCITOTENV.2020.143195.
[41] Coles D, et al. A review of the UK and British channel Islands practical tidal stream energy resource. Proc R Soc A Nov. 2021;477(2255). https://doi.org/10.1098/RSPA.2021.0469.
[42] Lewis M, Neill SP, Robins PE, Hashemi MR. Resource assessment for future generations of tidal-stream energy arrays. Energy Apr. 2015;83:403–15. https://doi.org/10.1016/J.ENERGY.2015.02.038.
[43] Wright Alasdair. Assessing the potential for low speed tidal stream energy generation in the UK. 2019 [Online]. Available: https://www.esru.strath.ac.uk/Documents/MSc_2019/Wright.pdf. [Accessed 15 January 2026].
[44] Tidal Stream Industry Energiser (Tiger). Tidal stream volume manufacturing roadmap document history. 2022 [Online]. Available: https://cms.ore.catapult.org.uk/wp-content/uploads/2023/03/EN-Volume-manufacture-roadmap-1.pdf. [Accessed 15 January 2026].
[45] Lewis M, Neill SP, Robins P, Hashemi MR, Ward S. Characteristics of the velocity profile at tidal-stream energy sites. Renew Energy Dec. 2017;114:258–72. https://doi.org/10.1016/J.RENENE.2017.03.096.
[46] Nova bluemull sound - appropriate assessment | tethys [Online]. Available: https://tethys.pnnl.gov/publications/nova-bluemull-sound-appropriate-assessment. [Accessed 7 August 2026].
[47] Paimpol-Bréhat - Fondation OPEN-C'. Accessed: August. 7, 2026. [Online]. Available: https://fondation-open-c.org/en/our-test-sites/paimpol-brehat/ .
[48] Pennock S, Noble DR, Vardanyan Y, Delahaye T, Jeffrey H. A modelling framework to quantify the power system benefits from ocean energy deployments. 2023. https://doi.org/10.7488/ds/7469.
[49] Brown T, Hörsch J, Schlachtberger D. PyPSA: python for power system analysis. J Open Res Software 2018;6(1). https://doi.org/10.5334/JORS.188.
[50] Staffell I, Pfenninger S. Using bias-corrected reanalysis to simulate current and future wind power output. Energy Nov. 2016;114:1224–39. https://doi.org/10.1016/J.ENERGY.2016.08.068.
[51] Pfenninger S, Staffell I. Long-term patterns of European PV output using 30 years of validated hourly reanalysis and satellite data. Energy Nov. 2016;114:1251–65. https://doi.org/10.1016/J.ENERGY.2016.08.060.
[52] Iain Staffell, Alex Pusey, Xie Judy Jingwei, Nathan Johnson. The global potential and hourly capacity factors of tidal range and tidal stream technologies. 2025.
[53] Egbert GD, Erofeeva SY. Efficient inverse modeling of barotropic ocean tides. J Atmos Ocean Technol 2002;19(2):183–204. https://doi.org/10.1175/1520-0426(2002)019<0183:EIMOBO>2.0.CO;2.
[54] Huang Z, Dai P, Zhang J. Joint development of tidal current energy in multi-channels surrounding Xiushan Island, China. Energy Mar. 2026;347:140327. https://doi.org/10.1016/J.ENERGY.2026.140327.
[55] Lewis M, et al. Power variability of tidal-stream energy and implications for electricity supply. Energy Sep. 2019;183:1061–74. https://doi.org/10.1016/J.ENERGY.2019.06.181.
[56] TECHNICAL SPECIFICATION marine energy-Wave, tidal and other water current converters-Part 201: tidal energy resource assessment and characterization. 2015 [Online]. Available: https://standards.iteh.ai/catalog/standards/sist/6317cad3-135a-4a43-9d47-. [Accessed 7 August 2026].
[57] Weatherall PA, et al. The GEBCO_2025 grid - a continuous terrain model for oceans and land at 15 arc-second intervals. Published Data Library (PDL) 2025. https://doi.org/10.5285/836F016A-33BE-6DDC-E053-6C86ABC0788E.
[58] Fairley I, Neill S, Wrobelowski T, Willis M, Masters I. Potential array sites for tidal stream electricity generation off the pembrokeshire Coast. 2011.
[59] Rosas-Chavoya M, Gallardo-Salazar JL, López-Serrano PM, Alcántara-Concepción PC, León-Miranda AK. QGIS a constantly growing free and open-source geospatial software contributing to scientific development. Cuadernos de Investigación Geográfica May 2022;48(1):197–213. https://doi.org/10.18172/cig.5143.
[60] Deb K, Pratap A, Agarwal S, Meyarivan T. A fast and elitist multiobjective genetic algorithm: NSGA-II. IEEE Trans Evol Comput Apr. 2002;6(2):182–97. https://doi.org/10.1109/4235.996017.
[61] Krityakierne T, Sinpayak P, Khiripet N. GIS spatial optimization for agricultural crop allocation using NSGA-II. Inf Process Agric Jun. 2025;12(2):139–50. https://doi.org/10.1016/J.INPA.2024.04.005.
[62] Blank J, Deb K. Pymoo: multi-objective optimization in python. IEEE Access 2020;8:89497–509. https://doi.org/10.1109/ACCESS.2020.2990567.
[63] NESO data portal [Online]. Available: https://www.neso.energy/data-portal. [Accessed 15 January 2026].
[64] Boyle J, Littler T, Foley A. Battery energy storage system state-of-charge management to ensure availability of frequency regulating services from wind farms. Renew Energy Nov. 2020;160:1119–35. https://doi.org/10.1016/J.RENENE.2020.06.025.
[65] 'Clean flexibility roadmap - GOV.UK'. Accessed: January. 21, 2026. [Online]. Available: https://www.gov.uk/government/publications/clean-flexibility-roadmap/clean-flexibility-roadmap.
[66] Li P, Wu W, Wang X, Xu B. A data-driven linear optimal power flow model for distribution networks. IEEE Trans Power Syst Jan. 2023;38(1):956–9. https://doi.org/10.1109/TPWRS.2022.3216161.
[67] Noble DR, Pennock S, Coles D, Delahaye T, Jeffrey H. Quantifying the system benefits of ocean energy in the context of variability: a UK example. Energies Jul. 2025;18(14):3717. https://doi.org/10.3390/EN18143717. 2025, Vol. 18, Page 3717.
[68] QGIS Development Team, 'QGIS Documentation (Version 3.40)'. Accessed: January. 15, 2026. [Online]. Available: https://docs.qgis.org/3.40/en/docs/index.html.
[69] Kang S, Li K, Wang R. A survey on pareto front learning for multi-objective optimization. J Membr Comput Sep. 2024;7(2):128–34. https://doi.org/10.1007/S41965-024-00170-Z. 2024 7:2.
[70] Jiang Q, Wang P. NSGA-II algorithm based control parameters optimization strategy for megawatt novel nuclear power systems. Energy Feb. 2025;316:134444. https://doi.org/10.1016/J.ENERGY.2025.134444.
[71] Abdulrazzaq AJ, Augie MA. Multi-objective optimization of hybrid renewable energy systems (Solar–Wind–Battery) for microgrids using an enhanced NSGA-II with uncertainty and carbon tax integration. SARC Publishers Aug. 2025;4(8):898–904. https://doi.org/10.5281/zenodo.16934242.
[72] Anand R, Aggarwal D, Kumar V. A comparative analysis of optimization solvers. J Stat Manag Syst Jul. 2017;20(4):623–35. https://doi.org/10.1080/09720510.2017.1395182.
[73] Zheng W, Doerr B. Mathematical runtime analysis for the non-dominated sorting genetic algorithm II (NSGA-II). Artif Intell Dec. 2023;325:104016. https://doi.org/10.1016/J.ARTINT.2023.104016.
[74] Schermeyer H, Vergara C, Fichtner W. Renewable energy curtailment: a case study on today's and tomorrow's congestion management. Energy Policy Jan. 2018;112:427–36. https://doi.org/10.1016/J.ENPOL.2017.10.037.
[75] Pavlík M, Bereš M, Kurimský F. Analyzing the impact of volatile electricity prices on solar energy capture rates in central Europe: a comparative study. Appl Sci Jul. 2024;14(15):6396. https://doi.org/10.3390/APP14156396. 2024, Vol. 14, Page 6396.
[76] Rostamnia N, Rashid TA. Investigating the effect of competitiveness power in estimating the average weighted price in electricity market. Electr J Oct. 2019;32(8):106628. https://doi.org/10.1016/J.TEJ.2019.106628.
[77] Copyright and licence | OpenStreetMap [Online]. Available: https://www.openstreetmap.org/copyright. [Accessed 12 October 2026].
[78] Mustapha MJ, Taylor G, Hulak D. A novel methodology to investigate the impact of electricity market reforms on future electricity prices. In: 2024 59th international universities power engineering conference (UPEC); 2024. p. 1–6. https://doi.org/10.1109/UPEC61344.2024.10892395.
[79] Strbac Goran, Aunedi Marko. Whole-system cost of variable renewables in future GB electricity system. 2016 [Online]. Available: http://energysuperstore.org/esrn/wp-content/uploads/2016/11/Whole-system-cost-of-variable-renewables-in-future-GB-electricity-system-Imperial_Nov2016.pdf. [Accessed 18 May 2026].
[80] Aunedi M, Pudjianto D, Strbac G. Calculating system integration costs of low-carbon generation technologies in future GB electricity system. IET Conference Publications 2016;2016(CP694). https://doi.org/10.1049/CP.2016.0529. CTYPE: STRING:BOOK.
[81] Teng F, Aunedi M, Strbac G. Benefits of flexibility from smart electrified transportation and heating in the future UK electricity system. Appl Energy Apr. 2016;167:420–31. https://doi.org/10.1016/J.APENERGY.2015.10.028.